REGULAR PAPER

J. Physiol. Sci. Vol. 56, No. 5; Oct. 2006; pp. 325–333
Online Sep. 9, 2006; **doi:10.2170/physiolsci.RP009006**

Baroreflex Increases Correlation and Coherence of Muscle Sympathetic Nerve Activity (SNA) with Renal and Cardiac SNAs

Atsunori KAMIYA, Toru KAWADA, Masaki MIZUNO, Tadayoshi MIYAMOTO, Kazunori UEMURA, Kenjiro SEKI, Shuji SHIMIZU, and Masaru SUGIMACHI

Department of Cardiovascular Dynamics, National Cardiovascular Centre Research Institute, Osaka, 565-8565 Japan

Abstract: Despite accumulating data of muscle sympathetic nerve activity (SNA) measured by human microneurography, whether neural discharges of muscle SNA correlates and coheres with those of other SNAs controlling visceral organs remains unclear. Further, how the baroreflex control of SNA affects the relations between these SNAs remains unknown. In urethane and α-chloralose anesthetized, vagotomized, and aortic-denervated rabbits, we recorded muscle SNA from the tibial nerve using microneurography and simultaneously recorded renal and cardiac SNAs. After isolating the carotid sinuses, we produced a baroreflex closed-loop condition by matching the isolated intracarotid sinus pressure (CSP) with systemic arterial pressure (CLOSE). We also fixed CSP at operating pressure (FIX) or altered CSP widely (WIDE: operating pressure ± 40 mmHg). Under these conditions, we calculated time-domain and frequency-domain measures of the correlation between muscle SNA and renal or cardiac SNAs. At CLOSE, muscle SNA resampled at 1 Hz correlated with both renal (r^2 = 0.71 ± 0.04, delay = 0.10 ± 0.004 s) and cardiac SNAs (r^2 = 0.58 ± 0.03, delay = 0.13 ± 0.004 s) at optimal delays. Moreover,muscle SNA at CLOSE strongly cohered with renal and cardiac SNAs(coherence >0.8) at the autospectral peak frequencies, and weakly (0.4–0.5) at the remaining frequencies. Increasing the magnitude of CSP change from FIX to CLOSE and further to WIDE resulted in corresponding increases in correlation and coherence functions at nonpeak frequencies, and the coherence functions at peak frequencies remained high (>0.8). In conclusion, muscle SNA correlates and coheres approximately with renal and cardiac SNAs under closed-loop baroreflex conditions. The arterial baroreflex is capable of potently homogenizing neural discharges of these SNAs by modulating SNA at the nonpeak frequencies of SNA autospectra.

Key words: sympathetic nerve activity, muscle, baroreflex.

Sympathetic nerve activity (SNA) has the crucial role of controlling circulation [1] and thus has been a major target in the research of circulatory physiology and pathophysiology. In humans, microneurography is the only direct method to measure SNA discharge [2]. By this technique, numerous human studies measured the activity of sympathetic nerves innervating the blood vessels in skeletal muscles (muscle SNA) [2–5] and used it as systemic SNA [3, 6–10]. However, since the measurable region in humans by this technique is almost limited to upper and lower extremities [2], the relation between muscle SNA and the SNAs controlling visceral organs such as the kidney and heart is not fully understood.

Arterial baroreflex is a major controller of SNA and thus may affect the relations between these SNAs. We previously reported that static-nonlinear and dynamic-linear baroreflex control of muscle SNA is similar to that of renal and cardiac SNAs under physiological pressure change in rabbits [11, 12]. Consistent with this finding, we have indeed observed that muscle SNA averaged over 1 minute parallels renal and cardiac SNAs in response to forced baroreceptor pressure change [11]. However, the relation between these SNAs in a time domain faster than 1 min and the relation in frequency domain remain unknown, despite the importance of their physiological and clinical relevance. First, the relation between these SNAs under conditions in which arterial pressure is regulated to normal level by a closed-loop baroreflex system is unclear. Next, the effects of baroreflex on the homogeneity in SNAs have not been analyzed quantitatively. Although canceling and enlarging the changes in baroreceptor pressure under open-loop baroreflex conditions are speculated to decrease and increase the homogeneity, respectively, how much muscle SNA correlates and coheres with other SNAs under these conditions remains unknown.

In the present study, we tested two hypotheses: (i) muscle SNA correlates and coheres with renal and cardiac SNAs under a closed-loop baroreflex condition, and (ii) the arterial baroreflex is capable of homogenizing neural discharges of these SNAs. In anesthetized rabbits with ca-

Received on Jul 27, 2006; accepted on Sep 6, 2006; released online on Sep 9, 2006; doi:10.2170/physiolsci.RP009006
Correspondence should be addressed to: Atsunori Kamiya, Department of Cardiovascular Dynamics, National Cardiovascular Centre Research Institute, Osaka 565-8565, Japan. Tel: +81-6-6833-5012; Fax: +81-6-6835-5403; E-mail: kamiya@ri.ncvc.go.jp

rotid sinuses isolated from systemic circulation, we simultaneously recorded muscle SNA from the tibial nerve by microneurography as well as renal and cardiac SNAs. We investigated the relation of muscle SNA with renal and cardiac SNAs under closed-loop baroreflex conditions and determined the proportions of the variance components of muscle SNA correlating and not correlating with renal and cardiac SNAs. Further, we also investigated these relations under two open-loop baroreflex conditions: fixed and widely fluctuating baroreceptor pressure.

MATERIALS AND METHODS

Surgical preparations. The animals were cared for in strict accordance with the Guiding Principles for the Care and Use of Animals in the Field of Physiological Sciences approved by the Physiological Society of Japan. Ten Japanese white rabbits weighing 2.4–3.3 kg were anesthetized by intravenous injection (2 ml/kg) of a mixture of urethane (250 mg/ml) and α-chloralose (40 mg/ml) and mechanically ventilated with oxygen-enriched room air. Supplemental anesthetics were injected as necessary (0.5 ml/kg) to maintain an appropriate level of anesthesia. We isolated the bilateral carotid sinuses vascularly from the systemic circulation by ligating the internal and external carotid arteries and other small branches originating from the carotid sinus regions. The isolated carotid sinuses were filled with warmed physiological saline through catheters inserted via the common carotid arteries. The intracarotid sinus pressure (CSP) was controlled by a servo-controlled piston pump (model ET-126A, Labworks; Costa Mesa, CA). Bilateral vagal and aortic depressor nerves were sectioned at the midlevel of the neck to eliminate baroreflexes from the cardiopulmonary region and the aortic arch. The systemic arterial pressure (AP) was measured using a high-fidelity pressure transducer (Millar Instruments; Houston, TX) inserted retrograde from the right common carotid artery below the isolated carotid sinus region. Body temperature was maintained at approximately 38°C with a heating pad.

We exposed the left renal sympathetic nerve retroperitoneally and the left cardiac sympathetic nerve through a middle thoracotomy. We attached a pair of stainless steel wire electrodes (Bioflex wire AS633, Cooner Wire) to each of these nerves to record renal and cardiac SNAs. To eliminate afferent signals, we tightly ligated and crushed the nerve fibers peripheral to the electrodes. To insulate and fix the electrodes, we covered the nerve and electrodes with a mixture of silicone gel (Silicon Low Viscosity, KWIK-SIL, World Precision Instrument, Inc., FL). We band-pass filtered the preamplified nerve signals at 150–1,000 Hz.

We exposed the left tibial nerve at the right popliteal fossa by incising the flexors of the dorsal middle thigh. We inserted a tungsten microelectrode (model 26-05-1, Federick Haer and Co., Bowdoinham, ME) to the right tibial nerve to record muscle SNA according to the microneurographic technique reported in humans [2, 13] and animals [14]. We identified muscle SNA according to the following discharge characteristics: (i) afferent activity being induced by tapping of the calf muscles but not by gently touching the skin, and (ii) excitatory and inhibitory responses to decreasing and increasing CSP, respectively. Then we tightly ligated and crushed the nerve fibers peripheral to the electrodes to eliminate afferent signals from the muscles. We fed the nerve signals into a preamplifier (Kohno Instruments, Nagoya) with active band-pass filters set from 480 to 5,000 Hz and continuously monitored these signals through a sound speaker.

We full-wave rectified and low-pass filtered the SNA signals with a cutoff frequency of 30 Hz to quantify the nerve activity. Pancuronium bromide (0.1 mg/kg) was administrated to prevent a contamination of muscular activity in these SNA recordings.

Protocols. After the surgical preparation, we kept the animal horizontally in a supine position. To test the first hypothesis that a neural discharge of muscle SNA parallels that of renal and cardiac SNAs, we measured the three SNAs while closing the baroreflex negative feedback loop by matching CSP with systemic AP (CLOSE protocol). We recorded CSP, SNAs, and systemic AP for 15 min at a sampling rate of 200 Hz, using a 12-bit analog-to-digital converter. After stabilizing the condition for at least 5 min, we recorded the data for 10 min and stored them on the hard disk of a dedicated laboratory computer system for later analysis. We also calculated the actual operating pressure by averaging systemic AP from the data.

To test the second hypothesis that baroreflex contributes to homogeneous sympathetic activation, we eliminated and greatly widened the baroreceptor pressure changes by the FIX and WIDE protocols, respectively, in baroreflex open-loop conditions. In the FIX protocol, we fixed CSP at the operating pressure [15, 16]. In the WIDE protocol, we randomly assigned CSP at 40 mmHg either above or below the operating pressure every 500 ms according to a binary white noise sequence [15, 17], where the input power spectrum of CSP was reasonably flat up to 1 Hz. The FIX and WIDE protocols were conducted serially in a randomized order at intervals of at least 5 min between protocols. During each protocol, we recorded measurements for 10 min and stored the data for analysis.

Data analysis. Under each baroreceptor pressure condition of CLOSE, WIDE, and FIX, we calculated the time domain (correlation coefficient) and frequency domain measures (coherence function) between muscle and renal or cardiac SNAs. In the time-domain analysis, we resampled SNA data at 1 Hz, assigned 100 arbitrary units (a.u.) to the maximal value during 10 min of CLOSE, and normalized other SNA signals to this value.

We scatter-plotted muscle SNA at 1 Hz against renal and cardiac SNAs with variable delays from renal and cardiac SNAs to muscle SNA (range: from 0 to 0.30 s at increments of 0.01 s) and calculated the correlation coefficient (r) [18] with optimal delays that maximized the square of correlation coefficient (r^2). The delays reflected the distances from the brain to the sites of measurement of these SNAs. The r^2 shows how perfectly a linear regression line describes the relationship between the two SNAs [19].

We also calculated the variance of muscle SNA resampled at 1 Hz [19]. The variance may include two components, one that correlates (correlative variance) and the other that does not correlate (noncorrelative variance) with other SNAs. Therefore we defined correlative and noncorrelative variance of muscle SNA to renal or cardiac SNA as follows (see APPENDIX) [18, 19]:

Correlative variance = SNA variance·r^2

Noncorrelative variance = SNA variance·$(1 - r^2)$

where SNA variance was the variance of muscle SNA, and r^2 was the correlation coefficient of muscle SNA against renal or cardiac SNA.

In the frequency-domain analysis, we calculated the coherence functions between muscle SNA and renal or cardiac SNA. We resampled SNA data at 10 Hz, and segmented them into 10 sets of 50% overlapping bins of 2^{10} data point each. SNA signals were similarly normalized as mentioned above. The segment length was 102.4 s, which yields the lowest frequency bound of 0.01 (0.0097) Hz. For each data set, we performed a fast Fourier transform while subtracting a linear trend and applying a Hanning window for each segment. We performed fast Fourier transform and ensemble averaged the power of muscle SNA [$S_{xx}(f)$], the power of renal or cardiac SNA [$S_{yy}(f)$], and the cross power between muscle SNA and renal or cardiac SNA [$S_{yx}(f)$] over the 10 segments. We derived a magnitude-squared coherence function [$Coh(f)$] of muscle SNA versus renal and cardiac SNAs as follows [17]:

$$Coh(f) = \frac{|S_{yx}(f)|^2}{S_{xx}(f)S_{yy}(f)}$$

The coherence value ranges from zero to unity. Unity coherence indicates a perfect linear correlation between muscle SNA and other SNAs, whereas zero coherence indicates total independence of the two SNAs. In an SNA autospectrum, when the power was three times greater than the averaged power of SNA from 0.01 to 1 Hz, we defined it as a peak. We separately calculated the averaged coherence function at the peak frequencies of muscle SNA autospectra and that at the remaining frequencies.

Statistic analysis. We presented all data as means ± SD. We used a repeated-measures analysis of variance with post hoc multiple comparisons to compare variables among experimental baroreceptor pressure conditions (FIX, CLOSE, WIDE) [19]. We considered differences significant when $P < 0.05$.

RESULTS

Relation between muscle SNA and cardiac or renal SNA in closed-loop baroreflex condition of CLOSE protocol

Time-domain analysis. In the CLOSE protocol (CSP matched with systemic arterial pressure), typical neural discharges of muscle SNA at 10 Hz appeared roughly the same as those of renal and cardiac SNAs (Fig. 1A). When the delay from renal and cardiac SNAs to muscle SNA was determined in individual animals to maximize r^2 (a typical example is shown in Fig. 1), muscle SNA resampled at 1 Hz correlated with both renal and cardiac SNAs with r^2 of 0.81 (delay = 0.10 s) and 0.64 (delay = 0.13 s), respectively (Fig. 1, B and C). The averaged data of all animals also showed that muscle SNA correlated with renal SNA ($r^2 = 0.71 \pm 0.04$, delay = 0.10 ± 0.004 s) and with

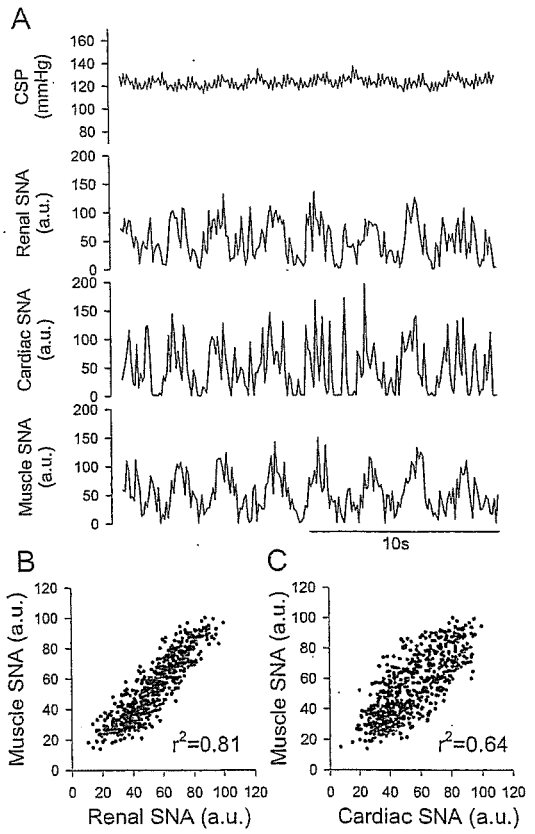

Fig. 1. (**A**) Representative time series for CSP, renal, cardiac, and muscle SNAs resampled at 10 Hz under the baroreflex closed-loop condition of CLOSE (CSP was matched to systemic AP). (**B**) Scatter plot of muscle SNA against renal SNA. (**C**) Scatter plot of muscle SNA against cardiac SNAs. The SNA signals were further resampled at 1 Hz. The delay from renal (0.10 s) or cardiac SNA (0.13 s) to muscle SNA was determined as the value that maximized r^2.

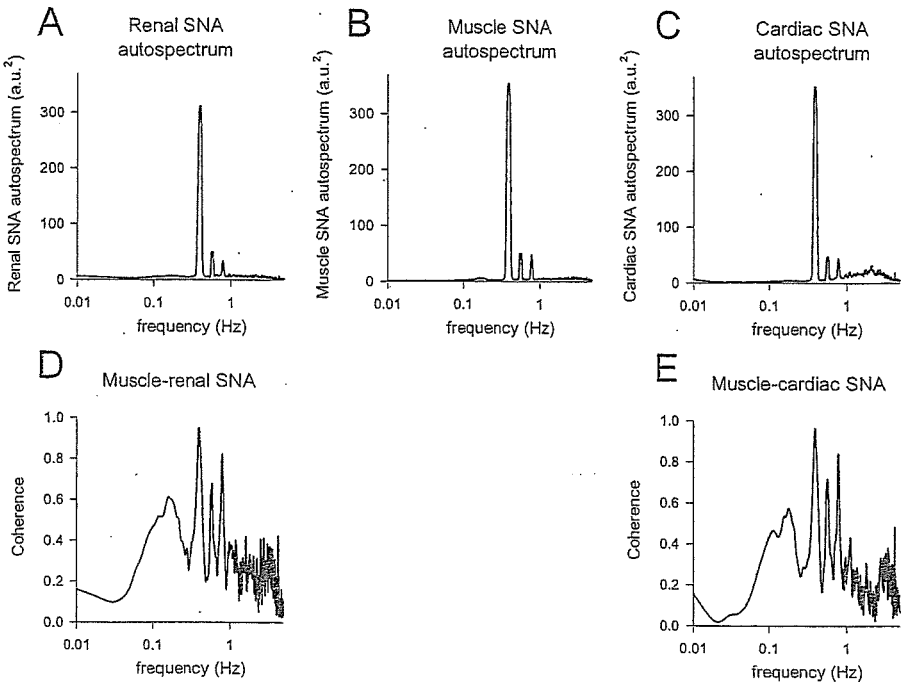

Fig. 2. Autospectra of renal (**A**), muscle (**B**), and cardiac SNAs (**C**) resampled at 1 Hz, and the coherence function of muscle SNA against renal (**D**) and cardiac SNAs (**E**) under the baroreflex closed-loop condition of CLOSE (CSP was matched to systemic AP), using the same data as in Fig. 1.

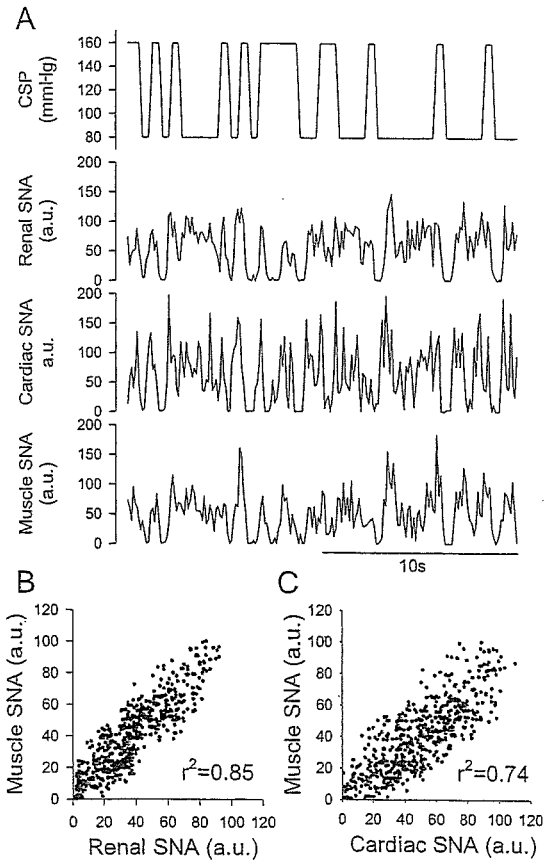

Fig. 3. (**A**) Representative time series for CSP, renal, cardiac, and muscle SNAs resampled at 10 Hz under the baroreflex open-loop condition of WIDE (CSP was varied according to a binary white noise sequence at 40 mmHg either above or below the operating pressure). (**B**) Scatter plots of muscle SNA resampled at 1 Hz against renal SNA (delay = 0.10 s). (**C**) Scatter plots of muscle SNA resampled at 1 Hz against cardiac SNA (delay = 0.13 s).

cardiac SNA (r^2 = 0.58 ± 0.03, delay = 0.13 ± 0.004 s) (Fig. 5, A and B). The r^2 was greater with renal than with cardiac SNA ($P < 0.05$). The pulse pressure of CSP was 30–40 mmHg.

Frequency-domain analysis. In the same animal as in Fig. 1, the autospectra of these SNAs showed a few peaks at common frequency ranges (Fig. 2, A, B, and C). Muscle SNA cohered with both renal and cardiac SNAs strongly at the peak frequencies of muscle SNA autospectra, but weakly at the remaining frequencies (Fig. 2, D and E). The individual animals all showed similar characteristics. The averaged coherence function of the animals was strong at the peak frequencies of the muscle SNA autospectrum (0.93 ± 0.01 between muscle and renal SNAs and 0.87 ± 0.02 between muscle and cardiac SNAs), but was weak at the remaining frequencies (0.5) (Fig. 8).

Effects of the magnitude of change in baroreceptor pressure on the relation between muscle SNA and cardiac or renal SNA

Time-domain analysis. In the same animal as in Fig. 1, the pattern of neural discharge of muscle SNA at 10 Hz resembled those of renal and cardiac SNAs to a greater extent in the WIDE protocol (CPS fluctuating between operating pressure ± 40 mmHg) (Fig. 3) than in the FIX protocol (CPS fixed at operating pressure) (Fig. 4). The correlation of muscle SNA resampled at 1 Hz with renal and cardiac SNAs was higher in WIDE (r^2 = 0.85, delay = 0.10 s, and r^2 = 0.74, delay = 0.13 s, respectively) (Fig. 3, B and C) than in CLOSE, but was lower in FIX (with the same delays, Fig. 4, B and C). Compared with CLOSE, the averaged data of all animals showed a higher correlation of muscle SNA with renal and cardiac SNAs in WIDE (r^2 = 0.79 ± 0.03, delay = 0.10 ± 0.004 s, and r^2 =

0.76 ± 0.02, delay = 0.13 ± 0.004 s, respectively), but lower correlation in FIX (r^2 = 0.53 ± 0.04, delay = 0.10 ± 0.004 s, and r^2 = 0.46 ± 0.04, delay = 0.13 ± 0.004 s, respectively) (Fig. 5, A and B). In WIDE, the r^2 was higher with renal than with cardiac SNA ($P < 0.05$). Similar results were observed when SNAs were resampled at slower and faster frequencies than 1 Hz (Fig. 6). In both SNA pairs, the r^2 was greater in WIDE than in CLOSE and FIX at frequencies from 0.01 to 5 Hz ($P < 0.05$), whereas it was greater in CLOSE than in FIX at frequencies from 0.3 to 5 Hz ($P < 0.05$).

The variance of muscle SNA sampled at 1 Hz increased from FIX to CLOSE and further to WIDE (Fig. 5, C and D; gray plus black column). The variance component of

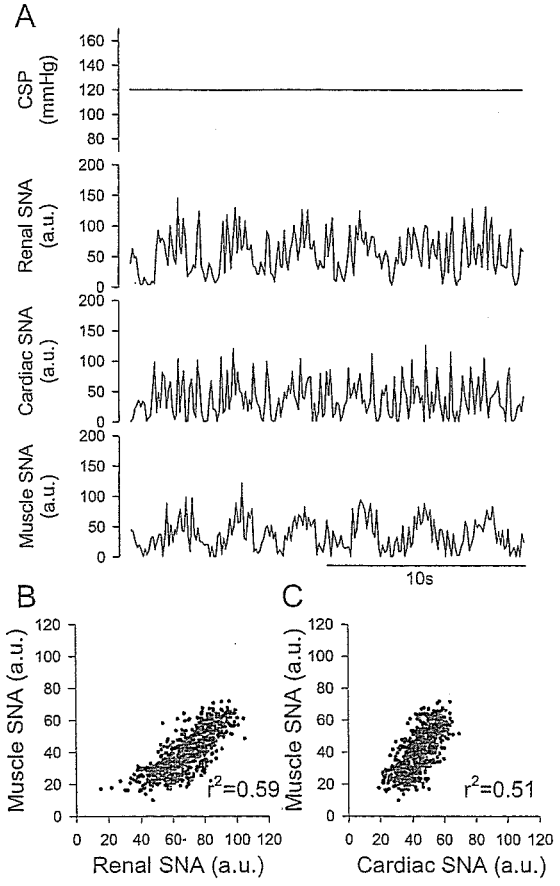

Fig. 4. (**A**) Representative time series for CSP, renal, cardiac, and muscle SNAs resampled at 10 Hz under the baroreflex open-loop condition of FIX (CSP was fixed at the operating pressure). (**B**) Scatter plot of muscle SNA resampled at 1 Hz against renal SNA (delay = 0.10 s). (**C**) Scatter plots of muscle SNA resampled at 1 Hz against cardiac SNA (delay = 0.13 s).

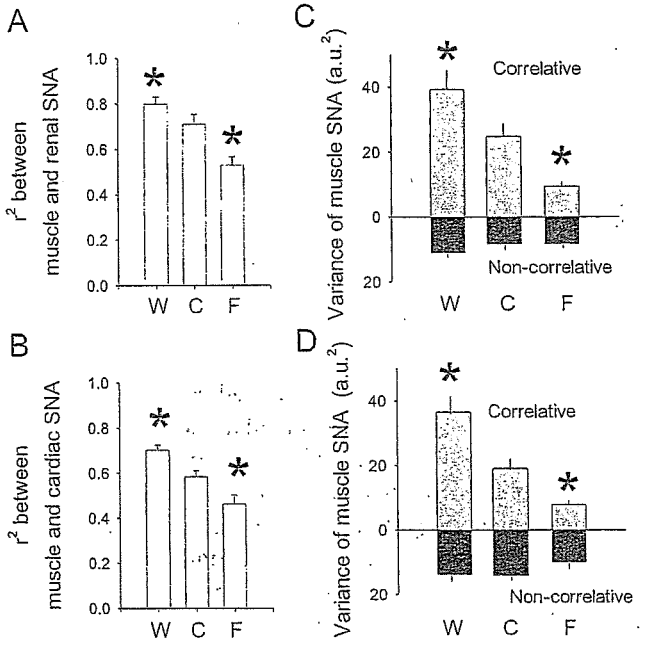

Fig. 5. The square of correlation coefficient (r^2) between muscle SNA resampled at 1 Hz and renal (**A**) or cardiac SNA (**B**) under baroreceptor pressure conditions of WIDE, CLOSE, and FIX. Floating columns show the averaged (±SD) correlative (gray top column) and noncorrelative (black bottom column) variance of muscle SNA versus renal (**C**) or cardiac SNA (**D**) resampled at 1 Hz in WIDE, CLOSE, and FIX. Correlative: variance component of muscle SNA correlating with other SNA; Noncorrelative: variance component of muscle SNA not correlating with other SNA; W: WIDE; C: CLOSE; F: FIX. *: $P < 0.05$, vs. CLOSE.

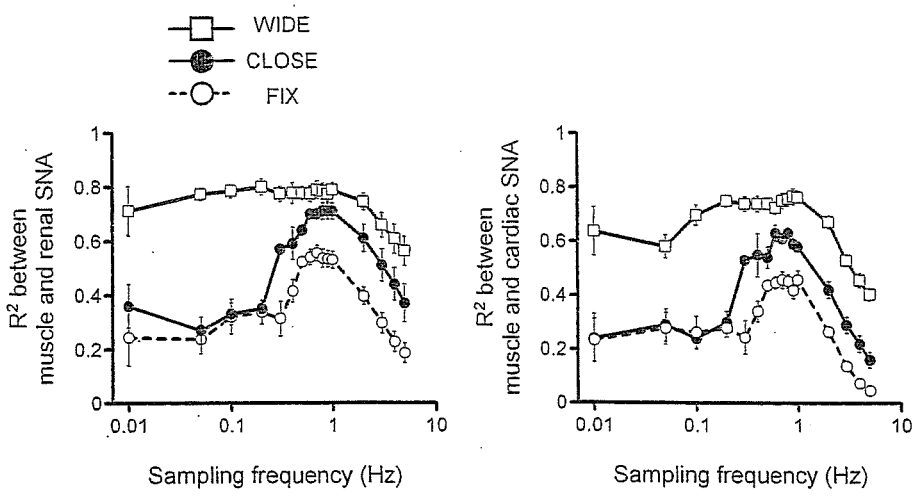

Fig. 6. The square of correlation coefficient (r^2) over SNA sampling frequency (0.01–5.0 Hz) between muscle SNA and renal (**A**) or cardiac SNA (**B**) under baroreceptor pressure conditions of WIDE (open square), CLOSE (closed circle), and FIX (open circle). In both SNA pairs, the r^2 was greater in WIDE than in CLOSE and FIX at frequencies observed ($P < 0.05$), whereas it was greater in CLOSE than in FIX at frequencies from 0.3 to 5.0 Hz ($P < 0.05$).

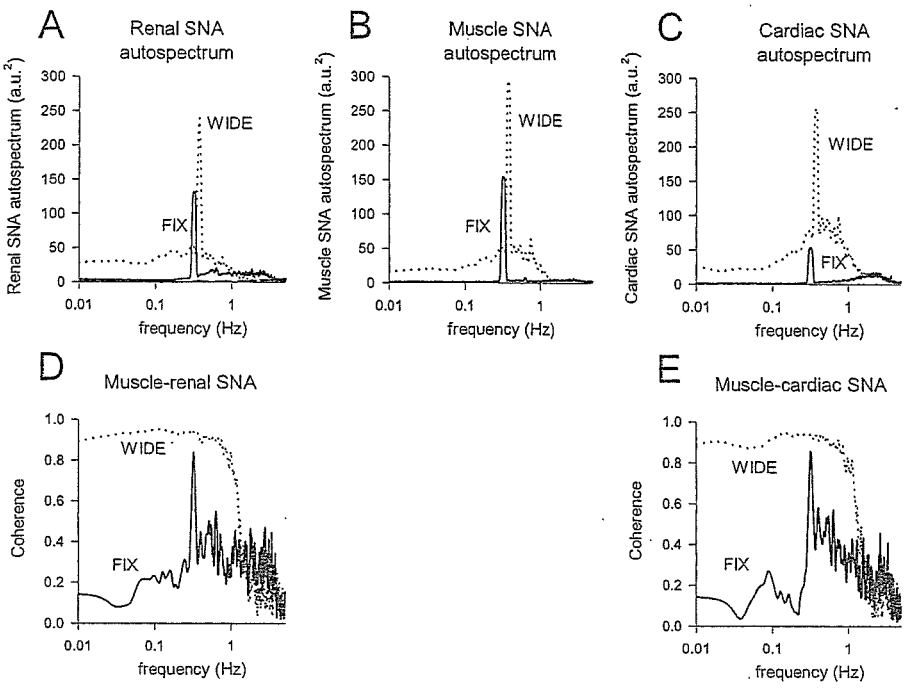

Fig. 7. Autospectra of renal (**A**), muscle (**B**), and cardiac SNAs (**C**), and the coherence function of muscle SNA against renal (**D**) and cardiac SNAs (**E**) under baroreflex open-loop conditions of WIDE (broken line) and FIX (solid line), using the same data as in Figs. 3 and 4.

muscle SNA that correlates with other SNAs, calculated as muscle SNA variance·r^2 ranked in the order of WIDE > CLOSE > FIX (Fig. 5, C and D; gray column), indicating a contribution of baroreflex-dependent regulation in maintaining homogeneity between muscle SNA and other visceral SNAs. In contrast, the variance component of muscle SNA that does not correlate with other SNAs, calculated as variance · $(1 - r^2)$, was similar among FIX, CLOSE, and WIDE (Fig. 5, C, D; black bottom column).

Frequency-domain analysis. In the same animal as in Fig. 1, the autospectra of muscle, renal, and cardiac SNAs peaked at exactly the same frequencies both in the WIDE and FIX protocols (Fig. 7, A, B, and C). Muscle SNA strongly cohered with both renal and cardiac SNAs both in WIDE and FIX at peak frequencies of the muscle SNA autospectra; however, the correlation was strong in WIDE but weak in FIX at the remaining frequencies (Fig. 7, D and E). The data of individual animals showed similar characteristics. The averaged coherence functions of all animals was consistently strong (>0.8) at peak frequencies of the muscle SNA autospectra regardless of baroreceptor pressure conditions of WIDE, CLOSE, and FIX (Fig. 8, black column). In contrast, the averaged coherence functions at the remaining frequencies were higher in WIDE (>0.8) compared with CLOSE or FIX (0.4–0.5) (Fig. 8, gray column).

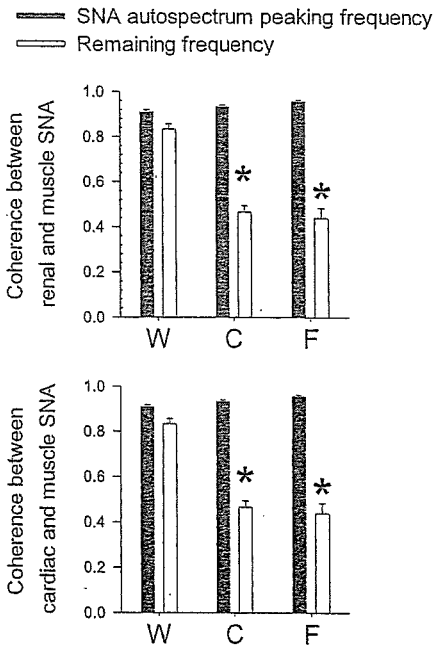

Fig. 8. Averaged coherence functions of muscle SNA against renal and cardiac SNAs at muscle SNA autospectral peak frequencies (black column) and at the remaining frequencies (gray column) under baroreceptor pressure conditions of WIDE, CLOSE, and FIX. W: WIDE; C: CLOSE; F: FIX. *P < 0.05, WIDE vs. CLOSE and FIX.

DISCUSSION

Despite the accumulating data on muscle SNA measured by microneurography in human studies, whether the neural discharge of muscle SNA correlates and coheres with that of other SNAs controlling visceral organs remains unclear. The major new findings in this study are (i) under the baroreflex closed-loop condition when CSP is matched with the systemic arterial pressure (CLOSE), muscle SNA resampled at 1 Hz correlates with both renal and cardiac SNAs in time-domain analysis (r^2: 0.6–0.7, with proper delay), and (ii) muscle SNA coheres with renal and cardiac SNAs in frequency domain analysis, particularly at peak frequencies of the SNA autospectra.

These results support our first hypothesis and indicate that muscle SNA correlates and coheres approximately with renal and cardiac SNAs under closed-loop baroreflex condition.

Next, although the baroreflex is known to strongly regulate muscles [3], renal and cardiac SNA [15, 20], the contribution of baroreflex to the homogeneous SNA discharges has not been elucidated quantitatively. The other major new findings in this study are as follows. When the change in baroreceptor pressure is increased from FIX (fixed CSP, no change) to CLOSE (CSP matching systemic arterial pressure, pulse pressure 30–40 mmHg) and further to WIDE (CSP fluctuating between ±40 mmHg), there are corresponding increases in the time domain correlation (r^2) of muscle SNA resampled at 1 Hz with renal and cardiac SNAs, from approximately 0.5 (FIX), to 0.6–0.7 (CLOSE), and to 0.8 (WIDE) (Fig. 5, A and B). The baroreflex dependent characteristics were also observed when SNAs were resampled at a frequency from 0.3 to 5.0 Hz (Fig. 6). This is also consistent with increases in the variance component of muscle SNA correlating with renal and cardiac SNAs (Fig. 5, C and D). These results agree with the concept that the baroreflex is important in generating harmonized SNA discharges [5, 21]. Moreover, the results indicate that arterial baroreflex has the ability to increase the homogeneity between these SNAs by nearly twofold. They support our second hypothesis and indicate that the arterial baroreflex potently homogenizes neural discharges of these SNAs.

Our results indicate that baroreflex increases the homogeneity between these SNAs by modulating SNA at nonpeak frequencies of SNA autospectra. The frequency domain correlation (coherence function) of muscle SNA with renal and cardiac SNAs was increased from approximately 0.4–0.5 (FIX), to 0.5 (CLOSE), to 0.9 (WIDE) at nonpeak frequencies, not peaking frequencies, of the SNA autospectra (Fig. 8). This suggests that other mechanisms other than baroreflex govern SNA at the nonpeak frequencies.

Our results quantitatively indicate that baroreflex-independent factors contribute to one-half of the homogeneity between muscle SNA and cardiac or renal SNA. Time-domain data show that even under a condition in which CSP is fixed at operating pressure, one-half of the variance of muscle SNAs correlates with other SNAs (Fig. 5, C and D; gray top column), with r^2 of approximately 0.5 (Fig. 5, A and B). These data indicate the presence of a baroreflex-independent component of SNA homogeneity. Although some noises may be included in the variance component of muscle SNA correlating with other SNAs, this is negligible in the calculation of variance, since the signal/noise ratio in SNA is >1,000 (noise was measured as the signal obtained after an individual animal died). The baroreflex-independent component of SNA homogeneity may be related to the strong coherence function between the SNAs at autospectral peak frequencies, since the coherence is consistently high regardless of the magnitude of baroreceptor pressure changes (Figs. 7, D and E, and 8). This component may partially be associated with the respiratory-related rhythm in sympathetic nerve discharge, a concept of central respiratory rhythm generator [21–23]. At the autospectral peak frequencies, these mechanisms may keep the coherence sufficiently high (0.9) independent of the baroreflex, and thus the baroreflex cannot increase the coherence further.

In contrast to the homogeneous sympathetic activation, the heterogeneity of muscle SNA versus renal or cardiac SNA does not relate with baroreflex. The proportions of the variance component of muscle SNA not correlating with renal and cardiac SNAs are constant regardless of the magnitude of change in baroreceptor pressure (Fig. 5, C and D). Mechanisms other than baroreflex may be involved in heterogeneous sympathetic activation. For example, chemoreflex [24], nitric oxide synthesis [25], and osmolarity [26] have been reported to produce regional differences in sympathetic activations.

Our data may strengthen the interpretation and the impact of the accumulated data on the involvement of human muscle SNA in circulatory physiology [3, 6–8, 10] and cardiovascular diseases [27, 28]. The recording of human microneurography is limited to the limbs, and there is so far little direct experimental evidence to support that muscle SNA parallel the other SNAs controlling visceral organs. The present study addresses this issue as an initial step and demonstrates the similarity between muscle SNA discharge and renal or cardiac SNA. Further study is needed to investigate the relations between SNAs in response to stimuli other than baroreflex.

Earlier studies have reported the coherence between pairs of SNA discharges for cardiac, renal, splanchnic, splenic, and lumbar SNAs in animals [29–31]. However, most of the studies focused on the coherence at frequencies faster than 1 Hz (0–15 Hz), in contrast to the present study. Furthermore, the previous studies did not measure muscle SNA or quantitatively investigate the effects of baroreflex on homogeneous SNA discharges.

Limitations

The present study has several limitations. First, anesthetic agents tend to inhibit efferent SNA and depress the gain of baroreflex control of SNA. Second, we excluded the efferent vagal nerve activities, which could affect SNA and baroreflex. Third, artificial respiration and surgical procedures used in this study may affect SNA and baroreflex. Last, based on most of the frequency domain studies of human muscle SNA [32–35], we focused on sympathetic discharge at frequencies of up to 1 Hz. And because of the low-pass characteristics of transfer function from SNA to arterial pressure (baroreflex peripheral arc) [20], the dynamic property of pressure response to

SNA becomes smaller as the frequency of SNA discharge increases. Future studies are needed to investigate the relation of muscle SNA with other SNAs at faster SNA rhythms, including a cardiac-related SNA rhythm at a frequency of 2 to 6 Hz [36] and an SNA rhythm of 10 Hz [37].

In conclusion, 1-Hz muscle SNA correlated with both renal and cardiac SNAs in time-domain analysis and cohered with renal and cardiac SNAs in frequency-domain analysis. Accompanying an increase in the magnitude of baroreceptor pressure change, both the correlation coefficient and the coherence function increased. These results indicate that muscle SNA correlates and coheres approximately with renal and cardiac SNAs under the closed-loop baroreflex condition and that the arterial baroreflex is capable of potently homogenizing neural discharges of these SNAs by modulating SNA at nonpeak frequencies of SNA autospectra.

APPENDIX

When y is scatter-plotted against x, a linear regression line can be drawn between the two variables. The Pearson product-moment correlation coefficient (r) between variables has the following relationship with variance (Eq. 1) [19]

$$r^2 = 1 - \frac{SS_{res}}{V_y} \quad (1)$$

where SS_{res} is the sum of squared deviations (residuals) from the regression line and V_y is the total sum of squared deviations from the mean of the dependent variable (y), that is, the total variance of y.

Equation 1 indicates that the square of correlation coefficient, r^2, is a fraction of the total variance in the dependent variable (y), which is explained by a linear regression relation [18, 19]. Equation 1 leads to the following relations in Eqs. 2 and 3.

$$V_y \cdot r^2 + SS_{res} = V_y \quad (2)$$

$$SS_{res} = V_y \cdot (1 - r^2) \quad (3)$$

$V_y \cdot r^2$ indicates the component of total variance in y that is explained by a linear regression relation (correlative variance in y). SS_{res} indicates the residual component of total variance in y that is not explained by linear regression relation (noncorrelative variance in y).

This study was supported by the Ground-based Research Announcement for Space Utilization project promoted by the Japan Space Forum, the research project promoted by the Ministry of Health, Labour and Welfare in Japan (#H18-nano-ippan-003), and the Grants-in-Aid for Scientific Research promoted by the Ministry of Education, Culture, Sports, Science and Technology in Japan (#18591992).

REFERENCES

1. Rowell LB. Human cardiovascular control. New York: Oxford Univ. Press; 1993.
2. Mano T. Microneurography as a tool to investigate sympathetic nerve responses to environmental stress. Aviakosmicheskaia i Ekologicheskaia Meditsina. 1997;31:8-14.
3. Wallin BG, Eckberg DL. Sympathetic transients caused by abrupt alterations of carotid baroreceptor activity in humans. Am J Physiol. 1982;242:H185-90.
4. Wallin BG, Esler M, Dorward P, Eisenhofer G, Ferrier C, Westerman R, *et al.* Simultaneous measurements of cardiac noradrenaline spillover and sympathetic outflow to skeletal muscle in humans. J Physiol (Lond). 1992;453:45-58.
5. Wallin BG, Thompson JM, Jennings GL, Esler MD. Renal noradrenaline spillover correlates with muscle sympathetic activity in humans. J Physiol (Lond). 1996;491:881-7.
6. Kamiya A, Michikami D, Fu Q, Niimi Y, Iwase S, Mano T, *et al.* Static handgrip exercise modifies arterial baroreflex control of vascular sympathetic outflow in humans. Am J Physiol Regul Integr Comp Physiol. 2001;281:R1134-9.
7. Markel TA, Daley JC, 3rd, Hogeman CS, Herr MD, Khan MH, Gray KS, *et al.* Aging and the exercise pressor reflex in humans. Circulation. 2003;107:675-8.
8. Mitchell JH, Victor RG. Neural control of the cardiovascular system: insights from muscle sympathetic nerve recordings in humans. Med Sci Sports Exerc. 1996;28(10 Suppl):S60-9.
9. Mosqueda-Garcia R, Furlan R, Tank J, Fernandez-Violante R. The elusive pathophysiology of neurally mediated syncope. Circulation. 2000;102:2898-906.
10. Tank J, Schroeder C, Diedrich A, Szczech E, Haertter S, Sharma AM, *et al.* Selective impairment in sympathetic vasomotor control with norepinephrine transporter inhibition. Circulation. 2003;107:2949-54.
11. Kamiya A, Kawada T, Yamamoto K, Michikami D, Ariumi H, Miyamoto T, *et al.* Muscle sympathetic nerve activity averaged over 1 minute parallels renal and cardiac sympathetic nerve activity in response to a forced baroreceptor pressure change. Circulation. 2005;112:384-6.
12. Kamiya A, Kawada T, Yamamoto K, Michikami D, Ariumi H, Miyamoto T, *et al.* Dynamic and static baroreflex control of muscle sympathetic nerve activity (SNA) parallels that of renal and cardiac SNA during physiological change in pressure. Am J Physiol Heart Circ Physiol. 2005;289:H2641-8.
13. Sundlof G, Wallin BG. Human muscle nerve sympathetic activity at rest. Relationship to blood pressure and age. J Physiol (Lond). 1978;274:621-37.
14. Nakamura T, Kawahara K, Kusunoki M, Feng Z. Microneurography in anesthetized rats for the measurement of sympathetic nerve activity in the sciatic nerve. J Neurosci Methods. 2003;131:35-9.
15. Kawada T, Shishido T, Inagaki M, Tatewaki T, Zheng C, Yanagiya Y, *et al.* Differential dynamic baroreflex regulation of cardiac and renal sympathetic nerve activities. Am J Physiol Heart Circ Physiol. 2001;280:H1581-90.
16. Kent BB, Drane JW, Blumenstein B, Manning JW. A mathematical model to assess changes in the baroreceptor reflex. Cardiology. 1972;57:295-310.
17. Marmarelis PZ, Marmarelis VZ. The whilte noise method in system identification. In: Analysis of Physiological Systems. New York: Plenum; 1978. p. 131-221.
18. Bendat JS, Piersol AG. Random data: analysis and measurement procedures. third edition. Canada: A Wiley-Interscience, 2000.
19. Glantz SA. Primer of biostatistics (4th ed.). New York: McGraw-Hill; 1997.
20. Ikeda Y, Kawada T, Sugimachi M, Kawaguchi O, Shishido T, Sato T, *et al.* Neural arc of baroreflex optimizes dynamic pressure regulation in achieving both stability and quickness. Am J Physiol. 1996;271:H882-90.
21. Habler HJ, Bartsch T, Janig W. Two distinct mechanisms generate the respiratory modulation in fibre activity of the rat cervical sympathetic trunk. J Auton Nerv Syst. 1996;61:116-22.
22. Morrison SF. Respiratory modulation of sympathetic nerve activity: effect of MK-801. Am J Physiol. 1996;270:R645-51.
23. Zhong S, Zhou SY, Gebber GL, Barman SM. Coupled oscillators account for the slow rhythms in sympathetic nerve discharge and phrenic nerve activity. Am J Physiol. 1997;272:R1314-24.
24. Iriki M, Dorward P, Korner PI. Baroreflex "resetting" by arterial hypoxia in the renal and cardiac sympathetic nerves of the rabbit. Pflugers Arch. 1977;370:1-7.
25. Hirai T, Musch TI, Morgan DA, Kregel KC, Claassen DE, Pickar JG, *et al.* Differential sympathetic nerve responses to nitric oxide synthase inhibition in anesthetized rats. Am J Physiol. 1995;269:R807-13.
26. Weiss ML, Claassen DE, Hirai T, Kenney MJ. Nonuniform sympathetic nerve responses to intravenous hypertonic saline infusion. J Auton Nerv Syst. 1996;57:109-15.
27. Macefield VG, Rundqvist B, Sverrisdottir YB, Wallin BG, Elam M. Firing properties of single muscle vasoconstrictor neurons in the sympathoexcitation associated with congestive heart failure. Circulation. 1999;100:1708-13.

28. Narkiewicz K, van de Borne PJ, Pesek CA, Dyken ME, Montano N, Somers VK. Selective potentiation of peripheral chemoreflex sensitivity in obstructive sleep apnea. Circulation. 1999;99:1183-9.
29. Kenney MJ, Barman SM, Gebber GL, Zhong S. Differential relationships among discharges of postganglionic sympathetic nerves. Am J Physiol. 1991;260:R1159-67.
30. Kenney MJ. Frequency characteristics of sympathetic nerve discharge in anesthetized rats. Am J Physiol. 1994;267:R830-40.
31. Kenney MJ, Weiss ML, Patel KP, Wang Y, Fels RJ. Paraventricular nucleus bicuculline alters frequency components of sympathetic nerve discharge bursts. Am J Physiol Heart Circ Physiol. 2001;281:H1233-41.
32. Eckberg DL. The human respiratory gate. J Physiol. 2003;548:339-52.
33. Kamiya A, Hayano J, Kawada T, Michikami D, Yamamoto K, Ariumi H, *et al.* Low-frequency oscillation of sympathetic nerve activity decreases during development of tilt-induced syncope preceding sympathetic withdrawal and bradycardia. Am J Physiol Heart Circ Physiol. 2005;289:H1758-69.
34. Furlan R, Porta A, Costa F, Tank J, Baker L, Schiavi R, *et al.* Oscillatory patterns in sympathetic neural discharge and cardiovascular variables during orthostatic stimulus. Circulation. 2000;101:886-92.
35. Van De Borne P, Montano N, Narkiewicz K, Degaute JP, Malliani A, Pagani M, *et al.* Importance of ventilation in modulating interaction between sympathetic drive and cardiovascular variability. Am J Physiol Heart Circ Physiol. 2001;280:H722-9.
36. Barman SM, Gebber GL. "Rapid" rhythmic discharges of sympathetic nerves: sources, mechanisms of generation, and physiological relevance. J Biol Rhythms. 2000;15:365-79.
37. Barman SM, Gebber GL, Zhong S. The 10-Hz rhythm in sympathetic nerve discharge. Am J Physiol. 1992;262:R1006-14.

REGULAR PAPER

J. Physiol. Sci. Vol. 56, No. 3; Jun. 2006; pp. 235–245
Online Jul. 7, 2006; **doi:10.2170/physiolsci.RP006006**

Sympathetic Neural Regulation of Heart Rate Is Robust against High Plasma Catecholamines

Toru KAWADA[1], Tadayoshi MIYAMOTO[1,2], Yuichiro MIYOSHI[1], Sayo YAMAGUCHI[1], Yukiko TANABE[1], Atsunori KAMIYA[1], Toshiaki SHISHIDO[1], and Masaru SUGIMACHI[1]

[1]Department of Cardiovascular Dynamics, Advanced Medical Engineering Center, National Cardiovascular Center Research Institute, Osaka, 565-8565 Japan; and [2]Japan Association for the Advancement of Medical Equipment, Tokyo, 113-0033 Japan

Abstract: The sympathetic regulation of heart rate (HR) may be attained by neural and humoral factors. With respect to the humoral factor, plasma noradrenaline (NA) and adrenaline (Adr) can reportedly increase to levels approximately 10 times higher than resting level during severe exercise. Whether such high plasma NA or Adr interfered with the sympathetic neural regulation of HR remained unknown. We estimated the transfer function from cardiac sympathetic nerve stimulation (SNS) to HR in anesthetized and vagotomized rabbits. An intravenous administration of NA (n = 6) at 1 and 10 $\mu g \cdot kg^{-1} \cdot h^{-1}$ increased plasma NA concentration (pg/ml) from a baseline level of 438 ± 117 (mean ± SE) to 974 ± 106 and 6,830 ± 917 ($P < 0.01$), respectively. The dynamic gain (bpm/Hz) of the transfer function did not change significantly (from 7.6 ± 1.2 to 7.5 ± 1.1 and 8.1 ± 1.1), whereas mean HR (in bpm) during SNS slightly increased from 280 ± 24 to 289 ± 22 ($P < 0.01$) and 288 ± 22 ($P < 0.01$). The intravenous administration of Adr (n = 6) at 1 and 10 $\mu g \cdot kg^{-1} \cdot h^{-1}$ increased plasma Adr concentration (pg/ml) from a baseline level of 257 ± 86 to 659 ± 172 and 2,760 ± 590 ($P < 0.01$), respectively. Neither the dynamic gain (from 8.0 ± 0.6 to 8.4 ± 0.8 and 8.2 ± 1.0) nor the mean HR during SNS (from 274 ± 13 to 275 ± 13 and 274 ± 13) changed significantly. In contrast, the intravenous administration of isoproterenol (n = 6) at 10 $\mu g \cdot kg^{-1} \cdot h^{-1}$ significantly increased mean HR during SNS (from 278 ± 11 to 293 ± 9, $P < 0.01$) and blunted the transfer gain value at 0.0078 Hz (from 5.9 ± 1.0 to 1.0 ± 0.4, $P < 0.01$). In conclusion, high plasma NA or Adr hardly affected the dynamic sympathetic neural regulation of HR.

Key words: systems analysis, neuro-humoral interaction, noradrenaline, adrenaline, isoproterenol.

The sympathetic regulation of heart rate (HR) may be attained by neural and humoral factors. One unique feature of the neural regulation, which is in contrast to the humoral regulation, is its quickness. The quickness of regulation may be best quantified by identifying dynamic characteristics of the input-output or stimulus-response relationship of a given system [1, 2]. Although we have identified the dynamic characteristics of the HR regulation by the cardiac sympathetic nerve by using a transfer function analysis [3, 4], we ignored the possible effects of plasma catecholamines on the transfer function. Plasma concentrations of noradrenaline (NA) and adrenaline (Adr) can increase during systemic sympathetic activation. For instance, plasma NA and Adr both increase to approximately 10 times their respective resting levels during severe exercise [5]. They increase to approximately 6 and 20 times, respectively, during acute myocardial infarction [5]. Whether such high plasma NA or Adr interfered with the dynamic sympathetic neural regulation of HR remained unanswered.

Two mutually opposing hypotheses can be put forward regarding interactions between the humoral and neural factors in the sympathetic regulation of HR. The activation of presynaptic (or prejunctional) α_2-adrenergic receptors located on the postganglionic sympathetic nerve terminals inhibits NA release [6], which would result in the attenuated HR response to cardiac sympathetic nerve stimulation (SNS). In contrast, the activation of presynaptic (or prejunctional) β_2-adrenergic receptors located on the postganglionic sympathetic nerve terminals facilitates NA release [7], which would result in the augmented HR response to cardiac SNS. Besides these interactions, high plasma NA can increase the cardiac uptake of NA [8], which would modify the HR response to cardiac SNS.

The aim of the present study was to test the hypothesis that high plasma NA or Adr alters the dynamic sympathetic neural regulation of HR. Using anesthetized rabbits, we examined the HR response to random cardiac SNS under the condition of elevated plasma NA or Adr induced by exogenous administration. We also examined the effects of an intravenous administration of a β-adrenergic agonist isoproterenol on the HR response to SNS. The results of

Received on Jun 1, 2006; accepted on Jul 4, 2006; released online on Jul 7, 2006; doi:10.2170/physiolsci.RP006006
Correspondence should be addressed to: Toru Kawada, Department of Cardiovascular Dynamics, Advanced Medical Engineering Center, National Cardiovascular Center Research Institute, 5-7-1 Fujishirodai, Suita, Osaka, 565-8565 Japan. Phone: +81-6-6833-5012 (Ext. 2427), Fax: +81-6-6835-5403, E-mail: torukawa@res.ncvc.go.jp

the present study indicated that high plasma NA or Adr hardly affected the dynamic sympathetic neural regulation of HR in anesthetized rabbits.

MATERIALS AND METHODS

Animal preparation. The animals were cared for in strict accordance with the Guiding Principles for the Care and Use of Animals in the Field of Physiological Sciences approved by the Physiological Society of Japan. Eighteen Japanese white rabbits weighing from 2.4 to 3.2 kg were anesthetized by a mixture of α-chloralose (40 mg/ml) and urethane (250 mg/ml), initiated with a bolus injection of 2 ml/kg and maintained with a continuous administration at 0.5 $ml \cdot kg^{-1} \cdot h^{-1}$. The rabbits were intubated and mechanically ventilated with oxygen-enriched room air. The right cardiac postganglionic sympathetic nerve was identified in the right thoracic cavity and sectioned. Usually, HR dropped immediately after the sectioning of the right cardiac sympathetic nerve, suggesting the importance of the right cardiac sympathetic nerve in determining baseline HR. A pair of platinum electrodes was attached to the cardiac end of the sectioned nerve for stimulation. The nerve and electrodes were secured by silicone glue (Kwik-Sil, World Precision Instruments, Sarasota, FL, USA). The left cardiac sympathetic nerve and other sympathetic branches to the heart were kept intact. The carotid sinus nerves and aortic depressor nerves were sectioned bilaterally to minimize changes in systemic sympathetic activity induced by baroreflexes. The vagal nerves were also sectioned bilaterally to eliminate the vagal effect on the heart. The vagotomy did not change HR significantly at this stage, possibly because of the vagolitic effects of the anesthesia. Arterial pressure (AP) was measured by a micromanometer (Millar Instruments, Houston, TX, USA) inserted into the thoracic aorta from the right femoral artery. HR was measured with a cardiotachometer (AT-601G, Nihon Kohden, Tokyo, Japan). An arterial catheter was inserted into the left femoral artery to sample blood for plasma catecholamine measurements. A double-lumen venous catheter was introduced into the right femoral vein for continuous anesthetic infusion and exogenous catecholamine administration.

Protocols. We quantified the dynamic sympathetic neural regulation of HR by using a transfer function analysis [3, 4]. To estimate the transfer function from cardiac SNS to HR, we dynamically stimulated the right cardiac sympathetic nerve as follows. The pulse duration was set at 2 ms, and the pulse amplitude was adjusted to obtain an HR increase of approximately 50 bpm (beats/min) during a 5-Hz constant stimulation in each animal. The resulting amplitude ranged from 0.8 to 2.0 V among animals. With these settings, the stimulation frequency was randomly assigned at either 0 or 5 Hz every 2 s, according to a binary white noise sequence (see appendix A for additional information). The average stimulation frequency was therefore 2.5 Hz. The input power spectral density of SNS was relatively flat up to 0.25 Hz.

In *Protocol 1* ($n = 6$), physiological saline was infused intravenously at 1 $ml \cdot kg^{-1} \cdot h^{-1}$ for 30 min after the end of surgical preparation (Fig. 1). A 300-μl volume of arterial blood was sampled under control conditions (designated as NA_0 condition) for plasma catecholamine measurements. Following the blood sampling, dynamic SNS was applied for 15 min to estimate the transfer function from SNS to HR. Arterial blood was sampled during the last minute of dynamic SNS under the NA_0 condition. Next, 1-μg/ml NA solution was infused at 1 $\mu g \cdot kg^{-1} \cdot h^{-1}$ (NA_1). Fifteen min after the initiation of NA_1 administration, when AP and HR had reached new steady states, arterial blood sampling and 15-min dynamic SNS were repeated. Third, a 10-μg/ml NA solution was administered at 10 $\mu g \cdot kg^{-1} \cdot h^{-1}$ (NA_{10}). Fifteen min after the initiation of NA_{10} administration, arterial blood sampling and 15-min dynamic SNS were repeated.

In *Protocol 2* ($n = 6$), experimental procedures similar to those in *Protocol 1* were conducted, using the Adr solution instead of the NA solution. The transfer function from SNS to HR was estimated under control condition (designated as Adr_0 condition), as well as during the administration of 1-μg/ml Adr solution at 1 $\mu g \cdot kg^{-1} \cdot h^{-1}$ (Adr_1) and 10-μg/ml Adr solution at 10 $\mu g \cdot kg^{-1} \cdot h^{-1}$ (Adr_{10}).

In *Protocol 3* ($n = 6$), we examined the effects of an intravenous administration of a β-adrenergic agonist isoproterenol on the transfer function from SNS to HR. Using experimental procedures similar to those in *Protocol 1*, we

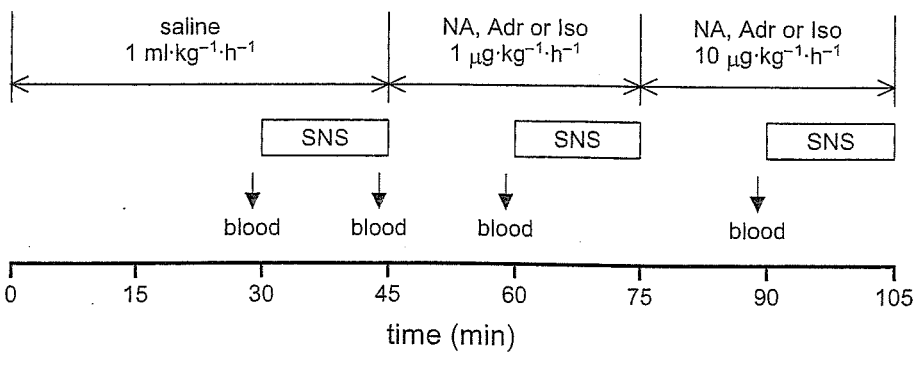

Fig. 1. Schematic diagram showing the experimental protocol. The downward arrows indicate the timings of blood sampling for catecholamine measurements (for *Protocols 1* and *2*). SNS: sympathetic nerve stimulation. NA: noradrenaline; Adr: adrenaline; Iso: isoproterenol.

administered 1-μg/ml isoproterenol solution at 1 μg·kg^{-1}·h^{-1} (Iso_1) and 10-μg/ml isoproterenol solution at 10 μg·kg^{-1}·h^{-1} (Iso_{10}) and estimated the transfer function under the control (designated as Iso_0), Iso_1, and Iso_{10} conditions.

Data analysis. The SNS command and HR were stored at a sampling rate of 200 Hz. The data were analyzed from only 2 min after the initiation of SNS to remove the initial trend of the HR increase. To estimate the transfer function from SNS to HR, we resampled the SNS-HR data pairs at 8 Hz. These data were segmented into 10 sets of half-overlapping bins of 1,024 data points each. In each segment, a linear trend was subtracted and a Hanning window was applied. The fast Fourier transform was then applied to obtain the frequency spectra of SNS and HR [9]. We calculated the ensemble averages of input power spectral density [$S_{SNS\cdot SNS}(f)$], output power spectral density [$S_{HR\cdot HR}(f)$], and cross-spectral density between the input and output [$S_{HR\cdot SNS}(f)$]. The transfer function [$H(f)$] was estimated using the following equation [10, 11].

$$H(f)=\frac{S_{HR\cdot SNS}(f)}{S_{SNS\cdot SNS}(f)} \tag{1}$$

We also calculated the magnitude-squared coherence function [$Coh(f)$] using the following equation [10, 11].

$$Coh(f)=\frac{\left|S_{HR\cdot SNS}(f)\right|^2}{S_{SNS\cdot SNS}(f)\,S_{HR\cdot HR}(f)} \tag{2}$$

The coherence function is a frequency-domain measure of the linear dependence between the input and output signals. A unity coherence value indicates a perfect linear dependence of HR on SNS, whereas a zero coherence value indicates the total independence between SNS and HR.

In *Protocols 1* and *2*, the transfer function from SNS to HR was parameterized by using a mathematical model [$H_m(f)$] of a second-order low-pass filter with pure dead time, using the following equation [3, 12].

$$H_m(f)=\frac{K}{1+2\zeta\frac{f}{f_N}j+\left(\frac{f}{f_N}j\right)^2}\exp(-2\pi f\,jL) \tag{3}$$

where K is the dynamic gain (in bpm/Hz), f_N is the natural frequency (in Hz), ζ is the damping ratio, and L is the pure dead time (in s); j represents the imaginary unit (see appendix B for details). A nonlinear iterative least square fitting was performed to minimize the following error function.

$$err=\frac{\sum_{i=1}^{N}\left|H(f_i)-H_m(f_i)\right|^2}{\sum_{i=1}^{N}\left|H(f_i)\right|^2},\ f_i=f_0\times i \tag{4}$$

where f_0 indicates the fundamental frequency of the Fourier transform. N specifies the upper frequency bound of the fitting procedure. We set N at 32 so as to fit $H_m(f)$ to $H(f)$ up to 0.25 Hz.

In *Protocol 3*, because the transfer function from SNS to HR during Iso_{10} was significantly deviated from the mathematical model of a second-order low-pass filter with pure dead time (Eq. 3), we did not fit the mathematical model to the transfer function and adopted the transfer gain values at the lowest frequency ($G_{0.0078}$) and at 0.1 Hz ($G_{0.1}$) to represent the frequency response of HR to SNS.

Catecholamine measurements. The arterial blood sample was centrifuged and a 100-μl volume of plasma was obtained. The plasma was transferred into a 1.5-ml polypropylene conical tube. A 50-μl volume of the working internal standard solution [100 pg of 3,4-dihydroxybenzylamine (DHBA)], 5 mg of acid-washed alumina, and 1.0 ml of 1-M tris(hydroxymethyl) aminomethane buffer (pH 8.6), containing 0.2% disodium ethylendiaminetetraacetic acid (EDTA), was added to the conical tube and shaken for 15 min. After shaking, the alumina was washed three times with distilled water, transferred into a microfilter (Ultrafree C3, Millipore, Bedford, MA), and centrifuged to remove excess fluid. NA, Adr, and DHBA were then eluted from the alumina, using 60 μl of 2% acetic acid, and their concentrations were measured by using high-performance liquid chromatography with electrochemical detection (DTA-300, Eicom, Kyoto, Japan). Plasma NA and Adr concentrations were calculated, taking into account the recovery rate of DHBA.

Statistical analysis. All data are presented in mean and mean ± SEM values. In *Protocol 1*, the effect of dynamic SNS on the plasma NA concentration was examined by a paired *t*-test under NA_0 condition. The NA and Adr concentrations before SNS were compared among NA_0, NA_1, and NA_{10} conditions, using Dunnett's test against a single control following the repeated-measures analysis of variance [13]. We also compared mean HR, mean AP, and parameters of the transfer function among NA_0, NA_1, and NA_{10} conditions, using Dunnett's test following repeated-measures analysis of variance. In *Protocol 2*, the effect of dynamic SNS on the plasma Adr concentration was examined by a paired *t*-test under Adr_0 condition. Other values, including plasma NA and Adr concentrations, mean HR, mean AP, and parameters of the transfer function, were compared among Adr_0, Adr_1, and Adr_{10} conditions, using Dunnett's test following repeated-measures analysis of variance. In *Protocol 3*, mean HR, mean AP, and gain values ($G_{0.0078}$ and $G_{0.1}$) were compared among Iso_0, Iso_1,

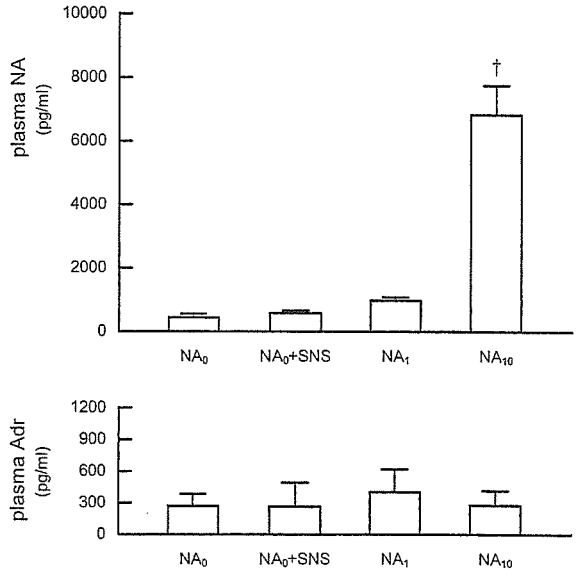

Fig. 2. Plasma concentrations of NA and Adr obtained from *Protocol 1*. The plasma NA concentration was significantly increased during the NA_{10} condition. The plasma Adr concentration was not changed significantly by the NA infusion. NA_0: saline infusion; NA_1 and NA_{10}: noradrenaline infusions at 1 and 10 $\mu g \cdot kg^{-1} \cdot h^{-1}$.

and Iso_{10} conditions, using Dunnett's test following repeated-measures analysis of variance. In all of the statistics, the difference was considered significant at $P < 0.05$.

RESULTS

Effects of high plasma NA on the dynamic sympathetic neural regulation of HR

In *Protocol 1*, dynamic SNS for 15 min did not change the plasma NA or Adr concentration significantly during NA_0 condition (Fig. 2, NA_0 vs. NA_0+SNS). The plasma NA concentration prior to dynamic SNS did not increase significantly during NA_1 condition, but increased to approximately 15 times higher during NA_{10} condition compared to NA_0 condition. The NA infusion did not significantly affect the plasma Adr concentration.

Figure 3A illustrates the time series of SNS, HR, and AP under NA_0, NA_1, and NA_{10} conditions obtained from one animal. The SNS was assigned at 0 or 5 Hz according to a binary white noise sequence. HR changed randomly in response to the dynamic SNS. Mean HR was slightly increased during NA infusion, whereas the amplitude of HR variation appeared unchanged. Mean AP was increased during NA_{10} condition compared to NA_0 condition.

Figure 3B shows averaged transfer functions from SNS to HR during NA_0, NA_1, and NA_{10} conditions obtained from all six animals in *Protocol 1*. The solid curve and the dashed curves in each plot represent mean and mean ± SEM values, respectively. In the gain plot, the transfer

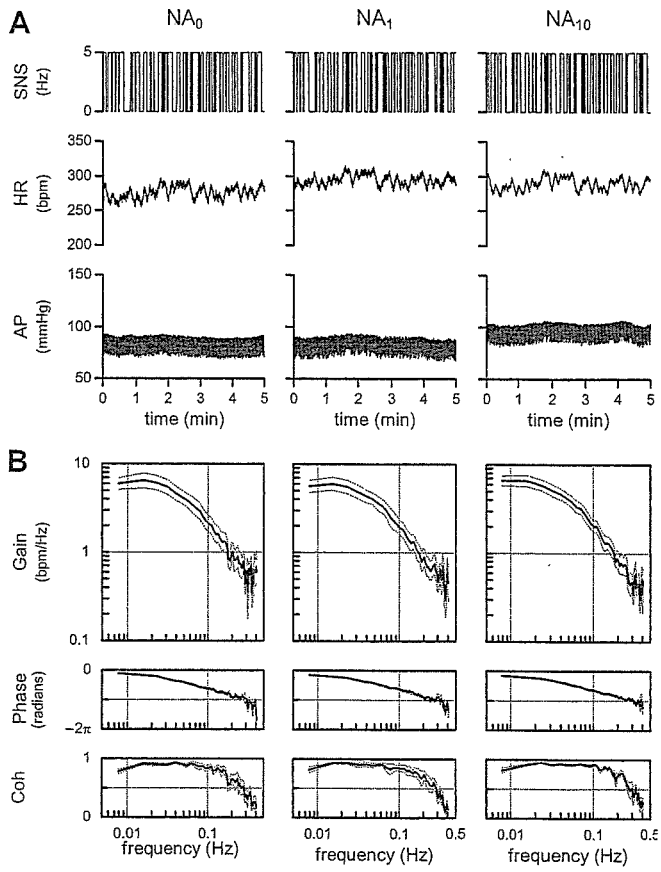

Fig. 3. A: Time series of one animal obtained from *Protocol 1*. Sympathetic nerve stimulation (SNS), heart rate (HR), and arterial pressure (AP) are shown. HR changed dynamically in response to SNS. **B**: Averaged transfer functions from SNS to HR during NA_0, NA_1, and NA_{10} conditions obtained from *Protocol 1* ($n = 6$). NA infusion did not affect the transfer function significantly except for changes in the damping ratio. Solid and dashed curves indicate mean and mean ± SEM values, respectively.

gain decreased with increasing frequency, reflecting the low-pass characteristics of the sympathetic neural regulation of HR. In the phase plot, the phase was near zero radians at the lowest frequency and delayed with increasing frequency, reflecting the SNS increases of HR. In the coherence plot, high coherence values up to 0.2 Hz indicate that approximately 80% of the HR variation in this frequency range was explained by the linear dynamics between SNS and HR. The transfer functions were similar among the three conditions. The dynamic gain, natural frequency, and pure dead time did not differ among the three conditions (Table 1). However, the damping ratio was significantly greater during NA_1 and NA_{10} conditions compared to the NA_0 condition.

Mean HR before SNS did not differ among NA_0, NA_1, and NA_{10} conditions, whereas mean HR during SNS increased significantly during NA_1 and NA_{10} conditions compared to NA_0 condition (Table 1). Although the repeated-measures analysis of variance indicated that the ef-

Table 1. Parameters obtained from *Protocol 1*.

	NA_0	NA_1	NA_{10}
HR, bpm			
Before SNS	248 ± 20	250 ± 19	251 ± 20
During SNS	280 ± 24	289 ± 22**	288 ± 22**
AP, mmHg			
Before SNS	95.7 ± 7.2	99.3 ± 8.1	106.6 ± 6.6*
During SNS	93.6 ± 8.0	102.9 ± 8.8**	106.0 ± 7.0**
Dynamic gain (K), bpm/Hz	7.6 ± 1.2	7.5 ± 1.1	8.1 ± 1.1
Natural frequency (f_N), Hz	0.080 ± 0.010	0.084 ± 0.010	0.083 ± 0.010
Damping ratio (ζ)	1.16 ± 0.05	1.48 ± 0.03*	1.52 ± 0.11*
Pure dead time (L), s	0.44 ± 0.08	0.55 ± 0.07	0.52 ± 0.06
Fitting error (err), %	1.6 ± 0.3	2.2 ± 0.6	1.6 ± 0.4

Values are means ± SEM. $^{**}P < 0.01$ and $^{*}P < 0.05$ vs. the corresponding value obtained during NA_0 condition. HR: heart rate. AP: arterial pressure. SNS: sympathetic nerve stimulation.

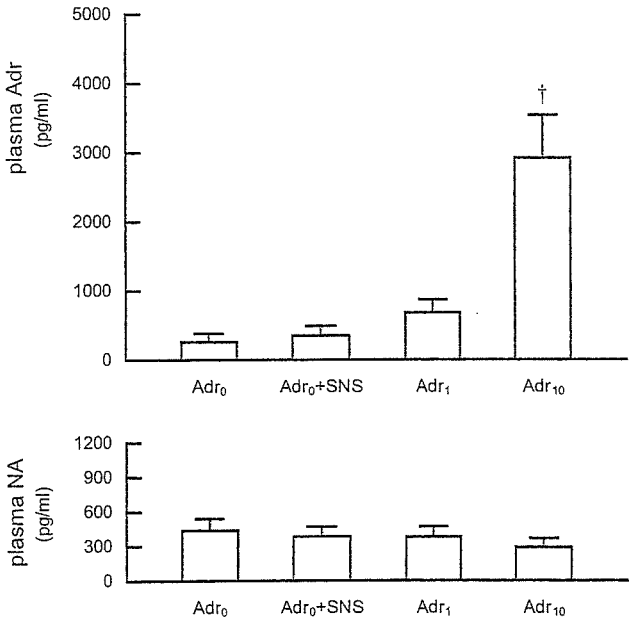

Fig. 4. Plasma concentrations of Adr and NA obtained from *Protocol 2*. The plasma Adr concentration was significantly increased during the Adr_{10} condition. The plasma NA concentration was not changed significantly by Adr infusion. Adr_0: saline infusion; Adr_1 and Adr_{10}: adrenaline infusions at 1 and 10 $\mu g \cdot kg^{-1} \cdot h^{-1}$.

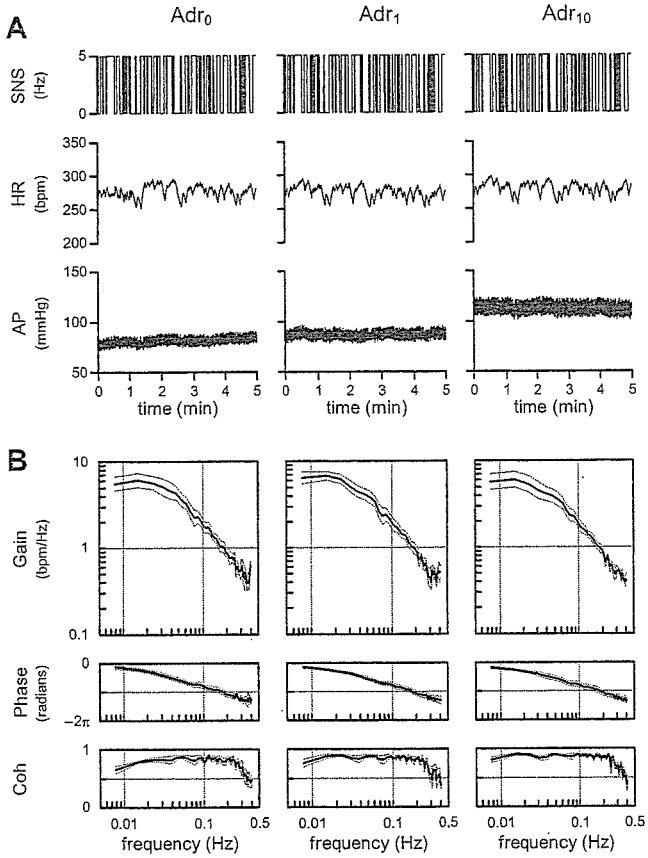

Fig. 5. A: Time series of one animal obtained from *Protocol 2*. HR changed dynamically in response to SNS. **B**: Averaged transfer functions from SNS to HR during Adr_0, Adr_1, and Adr_{10} conditions obtained from *Protocol 2* ($n = 6$). Adr infusion did not affect the transfer function significantly. Solid and dashed curves indicate mean and mean ± SEM values, respectively.

fects of NA infusion on mean HR during SNS were significant, the magnitude of the HR increase was small relative to the interindividual variation of HR. Mean AP before SNS was significantly elevated during NA_{10} condition, but not during NA_1 condition compared to NA_0 condition. Mean AP during SNS was increased significantly during both NA_1 and NA_{10} conditions compared to NA_0 condition.

Table 2. Parameters obtained from *Protocol 2*.

	Adr_0	Adr_1	Adr_{10}
HR, bpm			
Before SNS	231 ± 12	232 ± 10	228 ± 7
During SNS	274 ± 13	275 ± 13	274 ± 13
AP, mmHg			
Before SNS	93.1 ± 9.7	99.0 ± 8.3	113.7 ± 5.2**
During SNS	101.3 ± 8.0	103.8 ± 8.4	116.6 ± 4.6**
Dynamic gain (K), bpm/Hz	8.0 ± 0.6	8.4 ± 0.8	8.2 ± 1.0
Natural frequency (f_N), Hz	0.070 ± 0.005	0.071 ± 0.005	0.067 ± 0.006
Damping ratio (ζ)	1.09 ± 0.20	1.32 ± 0.11	1.39 ± 0.17
Pure dead time (L), s	0.55 ± 0.13	0.66 ± 0.09	0.63 ± 0.15
Fitting error (err), %	2.5 ± 0.5	1.8 ± 0.3	2.3 ± 0.6

Values are means ± SEM. **$P < 0.01$ vs. the corresponding value obtained during Adr_0 condition. HR: heart rate. AP: arterial pressure. SNS: sympathetic nerve stimulation.

Effects of high plasma Adr on the dynamic sympathetic neural regulation of HR

In *Protocol 2*, dynamic SNS for 15 min did not significantly change the plasma Adr or NA concentration during Adr_0 condition (Fig. 4, Adr_0 vs. Adr_0+SNS). The plasma Adr concentration prior to dynamic SNS did not increase significantly during Adr_1 condition, but increased to approximately 11 times higher during Adr_{10} condition compared to Adr_0 condition. The Adr infusion did not significantly affect the plasma NA concentration.

Figure 5A illustrates the time series of SNS, HR, and AP during Adr_0, Adr_1, and Adr_{10} conditions obtained from one animal. HR changed randomly in response to the dynamic SNS. The Adr infusion did not significantly change mean HR or the amplitude of HR variation among Adr_0, Adr_1, and Adr_{10} conditions. Mean AP increased during Adr_{10} condition compared to the Adr_0 condition.

Figure 5B shows averaged transfer functions from SNS to HR during Adr_0, Adr_1, and Adr_{10} conditions obtained from all of the six animals in *Protocol 2*. There seem to be no effects of Adr infusion on the transfer functions. No significant differences in dynamic gain, natural frequency, damping ratio, and pure dead time were observed among the three conditions (Table 2).

Mean HR did not differ significantly among Adr_0, Adr_1, and Adr_{10} conditions, both before and during SNS (Table 2). Mean AP increased significantly during Adr_{10} condition, but not during Adr_1 condition compared with Adr_0 condition, both before and during SNS.

Effects of intravenous isoproterenol on the dynamic sympathetic neural regulation of HR

Figure 6A illustrates the time series of SNS, HR, and AP during Iso_0, Iso_1, and Iso_{10} conditions obtained from one animal. HR changed randomly in response to the dynamic SNS under the Iso_0 condition. Although the dynamic HR response to SNS was maintained under the Iso_1 condition, mean HR was significantly elevated, and no apparent HR response was observed under the Iso_{10} condition.

Figure 6B shows averaged transfer functions from SNS to HR during Iso_0, Iso_1, and Iso_{10} conditions obtained from all of the six animals in *Protocol 3*. The transfer function showed a slight downward shift under the Iso_1 condition compared to the Iso_0 condition. It was significantly deformed and lost consistent characteristics across the animals under the Iso_{10} condition, as evidenced by large standard errors (dashed lines). The gain values ($G_{0.0078}$ and $G_{0.1}$) were significantly lower under the Iso_{10} condition compared to the Iso_0 condition (Table 3).

Mean HR did not change significantly under the Iso_1 condition, but increased significantly under the Iso_{10} condition compared to that under the Iso_0 condition, both before and during SNS (Table 3). Mean AP before SNS was significantly increased under the Iso_1 condition, but not under the Iso_{10} condition compared to that under the Iso_0 condition. Mean AP during SNS did not differ under the Iso_1 condition, but decreased significantly under the Iso_{10} condition compared to that under the Iso_0 condition.

DISCUSSION

We have examined the effects of high plasma NA or Adr on the transfer function from SNS to HR and found that high plasma catecholamines within physiological limits (approximately 10 times the resting levels) were ineffective to alter the sympathetic neural regulation of HR. Although the baseline HR was higher than the resting HR reported in conscious rabbits, the high baseline HR may be partly due to vagotomy. Because dynamic SNS (average stimulation frequency was 2.5 Hz) could increase mean HR, on the average, by 32 bpm in *Protocol 1* and by 43 bpm in *Protocol 2* under control conditions (NA_0 and Adr_0), the insignificant effects of high plasma catecholamines on HR cannot be explained by a simple saturation

Table 3. Parameters obtained from *Protocol 3*.

	Iso_0	Iso_1	Iso_{10}
HR, bpm			
Before SNS	244 ± 7	245 ± 6	289 ± 8**
During SNS	278 ± 11	280 ± 10	293 ± 9**
AP, mmHg			
Before SNS	80.2 ± 8.5	96.2 ± 4.9*	83.5 ± 7.1
During SNS	90.9 ± 7.4	93.1 ± 7.4	82.9 ± 7.0**
$G_{0.0078}$, bpm/Hz	5.9 ± 1.0	4.7 ± 0.8	1.0 ± 0.4**
$G_{0.1}$, bpm/Hz	1.3 ± 0.3	0.9 ± 0.2	0.2 ± 0.2**

Values are means ± SEM. $^{**}P < 0.01$ and $^{*}P < 0.05$ vs. the corresponding value obtained during Iso_0 condition. HR: heart rate. AP: arterial pressure. SNS: sympathetic nerve stimulation. $G_{0.0078}$: transfer gain value at 0.0078 Hz. $G_{0.1}$: transfer gain value at 0.1 Hz.

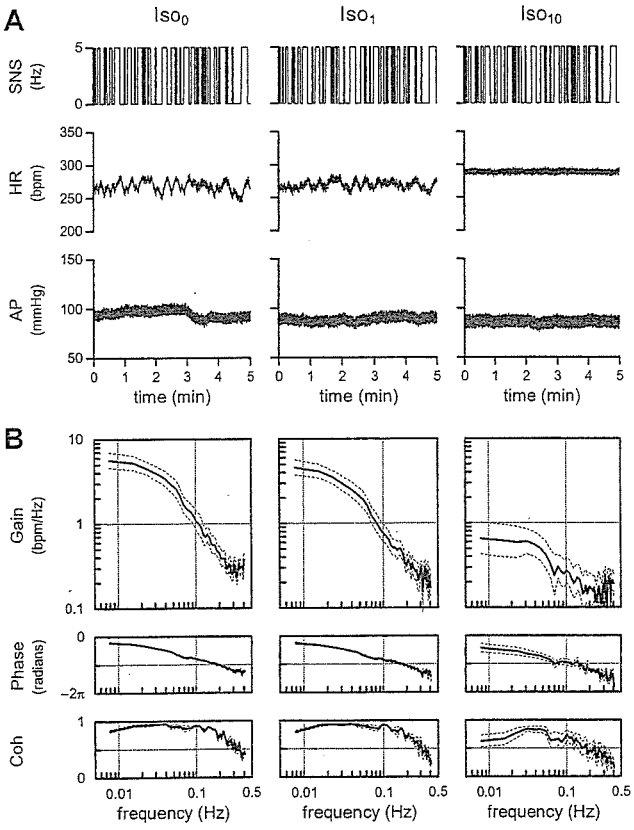

Fig. 6. A: Time series of one animal obtained from *Protocol 3*. Although HR changed dynamically in response to SNS under Iso_0 and Iso_1 conditions, mean HR elevated significantly, and no apparent dynamic HR response was observed under the Iso_{10} condition. **B**: Averaged transfer functions from SNS to HR during Iso_0, Iso_1, and Iso_{10} conditions obtained from *Protocol 3* (n = 6). The transfer gain reduced significantly and varied among animals, as evidenced by the large SEM under the Iso_{10} condition. Solid and dashed curves indicate mean and mean ± SEM values, respectively. Iso_0: saline infusion; Iso_1 and Iso_{10}: isoproterenol infusions at 1 and 10 $\mu g \cdot kg^{-1} \cdot h^{-1}$.

phenomenon of the HR response to catecholamines or by complete downregulation of β-adrenergic receptors under the present experimental settings. Actually, we confirmed that the same dose of intravenous administration of a β-adrenergic agonist isoproterenol increased mean HR significantly and blunted the transfer function (Fig. 6, Iso_{10} in *Protocol 3*). It is quite likely that NA released from the sympathetic nerve terminals during SNS has much stronger effects on HR in comparison with circulating catecholamines.

Effects of high plasma NA on the sympathetic neural regulation of HR

The plasma NA concentration increased approximately 15 times higher during NA_{10} condition than during NA_0 condition. Nevertheless, mean HR before SNS did not change significantly during NA_{10} condition compared to NA_0 condition (Table 1). In contrast, mean AP before SNS increased significantly during NA_{10} condition compared to NA_0 condition (Table 1). Young *et al.* [14] also reported an increase in AP and no changes in HR during NA infusion at 0.2 $\mu g \cdot kg^{-1} \cdot min^{-1}$ (12 $\mu g \cdot kg^{-1} \cdot h^{-1}$) in conscious dogs, though the baroreflexes could have counteracted the potential increase of HR in their study. These results indicate that the vascular bed is more responsive to plasma NA than the sinus node. A tighter synaptic cleft of the neuroeffector junction of the cardiac muscle compared to the vasculature, though it was reported in rat tissues [15], might explain the differential sensitivity to plasma NA between HR and AP.

Cardiac SNS significantly increased the mean HR without increasing the plasma NA concentration (Fig. 2), consistent with previous studies in anesthetized dogs [16] and cats [17]. Although mean HR before SNS did not differ among NA_0, NA_1, and NA_{10} conditions, mean HR during SNS was significantly higher during NA_1 and NA_{10} conditions compared to control (Table 1). These results are in opposition to the hypothesis that high plasma NA activates presynaptic α_2-adrenergic receptors and attenuates the HR response to SNS. One possible explanation for the increased mean HR during SNS under conditions of the NA infusion is as follows. NA released from the sympathetic nerve terminals is removed from the synaptic cleft by two catecholamine uptake mechanisms: a high-affinity, low-capacity neuronal uptake ($uptake_1$) and a low-affinity, high-capacity extraneuronal uptake ($uptake_2$) [5,

18, 19]. The uptake$_1$ mechanism also contributes to plasma clearance of NA [20]. High plasma NA might occupy the uptake$_1$ process to some extent and slow the NA removal from the synaptic cleft during SNS. As a result, the positive chronotropic effects of SNS might be augmented. Honda *et al.* [8] investigated the relationship between the kinetics of plasma catecholamines and cardiac sympathetic nerve activity during systemic hypotension induced by vena cava occlusion. They showed that the cardiac uptake of NA proportionally increased as the arterial NA concentration increased and that there was a negative correlation between the cardiac uptake of NA and the percent increase in mean cardiac sympathetic nerve activity. The negative correlation between the cardiac uptake of NA and the percent increase in mean cardiac sympathetic nerve activity might support the notion that NA of plasma origin and that of neural origin share the uptake$_1$ process. Although the within-individual change was statistically significant, the magnitude of HR increase during SNS was small compared to the interindividual variation of mean HR. Therefore the augmentation of the positive chronotropic effects by high plasma NA may be physiologically insignificant.

In the transfer function parameters, the damping ratio alone was significantly increased during NA_1 and NA_{10} conditions compared with NA_0 condition (Table 1). As already discussed, high plasma NA might have interfered with the uptake$_1$ process and consequently changed the damping ratio of the transfer function [12]. The damping ratio is an important determinant of the system behavior of the second-order low-pass filter. Depending on the value of the damping ratio, the system behaves as underdamped ($0 < \zeta < 1$), critically damped ($\zeta = 1$), or overdamped ($\zeta > 1$) (see appendix B). In the present study, however, the damping ratios changed only from 1.2 to 1.5; thus the system should behave as over-damped under any of the NA_0, NA_1, and NA_{10} conditions. Given that other transfer function parameters including the dynamic gain, natural frequency, and pure dead time did not change significantly, high plasma NA has limited effects on the transfer function from SNS to HR.

Effects of high plasma Adr on the sympathetic neural regulation of HR

The plasma Adr concentration during Adr_{10} condition increased to approximately 11 times that during Adr_0 condition. Although high plasma Adr did not increase HR, it did increase AP (Table 2). In contrast, Young *et al.* [14] reported that an administration of Adr at 0.2 $\mu g \cdot kg^{-1} \cdot min^{-1}$ (12 $\mu g \cdot kg^{-1} \cdot h^{-1}$) significantly increased both AP and HR in conscious dogs. Since the plasma Adr concentration in their study increased to a similar degree to the present result, the HR response to plasma Adr may differ between rabbits and dogs. Other factors that potentially explain the discrepancy are the vagotomy and anesthesia used in the present study. On the other hand, the Adr administration could have altered cardiac sympathetic neural outflow in the study by Young *et al.* [14].

In the present experimental conditions, high plasma Adr did not increase mean HR during SNS compared to Adr_0 condition and did not affect the transfer function from SNS to HR either (Table 2). These results are in opposition to the hypothesis that high plasma Adr activates presynaptic β_2-adrenergic receptors and augments the HR response to SNS. Moreover, because Adr has lower affinity to the uptake$_1$ process compared to NA [18, 19], high plasma NA but not Adr affected the mean HR during SNS and the damping ratio of the transfer function via the mechanism of modulating the NA removal.

The present results are consistent with the study of Boudreau *et al.* [21], in which a 10-min administration of Adr (92 $ng \cdot kg^{-1} \cdot min^{-1}$ or 5.5 $\mu g \cdot kg^{-1} \cdot h^{-1}$) did not increase the NA release in response to cardiac SNS in anesthetized dogs. However, Boudreau *et al.* [21] also demonstrated that a 180-min administration of Adr did increase the NA release in response to cardiac SNS, along with an increased Adr level in the cardiac tissue. Plasma Adr can be taken up into the sympathetic nerve terminals and then coreleased with NA [22]. When Adr is coreleased with NA into the synaptic cleft, NA release may be facilitated via the presynaptic β_2-adrenergic mechanism because Adr is a more potent agonist for β_2-adrenergic receptors than NA [23]. Although the long-term effects of high plasma Adr on the transfer function from SNS to HR was not examined in the present study, it is conceivable that high plasma Adr does not affect the sympathetic neural regulation of HR unless the Adr accumulation in the sympathetic nerve terminals reaches a concentration that is high enough.

Effects of intravenous isoproterenol on the dynamic sympathetic neural regulation of HR

As expected, an intravenous administration of isoproterenol at 10 $\mu g \cdot kg^{-1} \cdot h^{-1}$ increased mean HR significantly both before and during SNS. The transfer gain of the HR response to SNS was significantly decreased under the Iso_{10} condition (Table 3). These results are similar to our previous finding that an increase in mean stimulation frequency of SNS increased mean HR and decreased the transfer gain [12]. We have explained a bidirectional augmentation of the dynamic HR response to autonomic nerve stimulation by using a nonlinear sigmoidal relationship between the autonomic tone and HR [3, 24]. In that concept, the operating point of HR critically affects the transfer gain of the HR response to sympathetic or vagal nerve stimulation; i.e., deviation of the operating point from the center of the sigmoidal relationship decreases the tangential line of the sigmoid curve that relates to the transfer gain. Such operating-point dependence of the transfer gain may explain, at least in part, the decrease in

the transfer gain under the Iso_{10} condition.

Several limitations need to be addressed. First, we performed the experiment in anesthetized rabbits. Because the anesthesia would affect the autonomic tone, the results may not be directly applicable to conscious animals. However, because we cut and stimulated the right cardiac sympathetic nerve, changes in autonomic outflow associated with anesthesia might not have significantly affected the present results. Second, as already mentioned, species differences in HR response to catecholamines may exist. Whether high plasma catecholamines affect the dynamic sympathetic neural regulation of HR in animal species other than rabbits requires further investigations. Third, the duration of catecholamine administration prior to SNS was set at 15 min. Although this priming time was sufficient for AP and HR to reach new steady states, the effects of longer durations of high plasma catecholamines on the dynamic sympathetic neural regulation of HR remain to be investigated. And fourth, because we stimulated the cardiac postganglionic sympathetic nerve, the possible effects of high plasma catecholamines on sympathetic ganglionic transmission were excluded.

In conclusion, although plasma NA or Adr were increased to a level 10–15 times higher than the baseline level by exogenous administration, such high plasma NA or Adr did not significantly affect the dynamic sympathetic neural regulation of HR in anesthetized rabbits. Although humoral and neural factors are thought to regulate the cardiovascular system in concert, the neural factor appears to be much stronger than the humoral factor as far as the HR regulation is concerned.

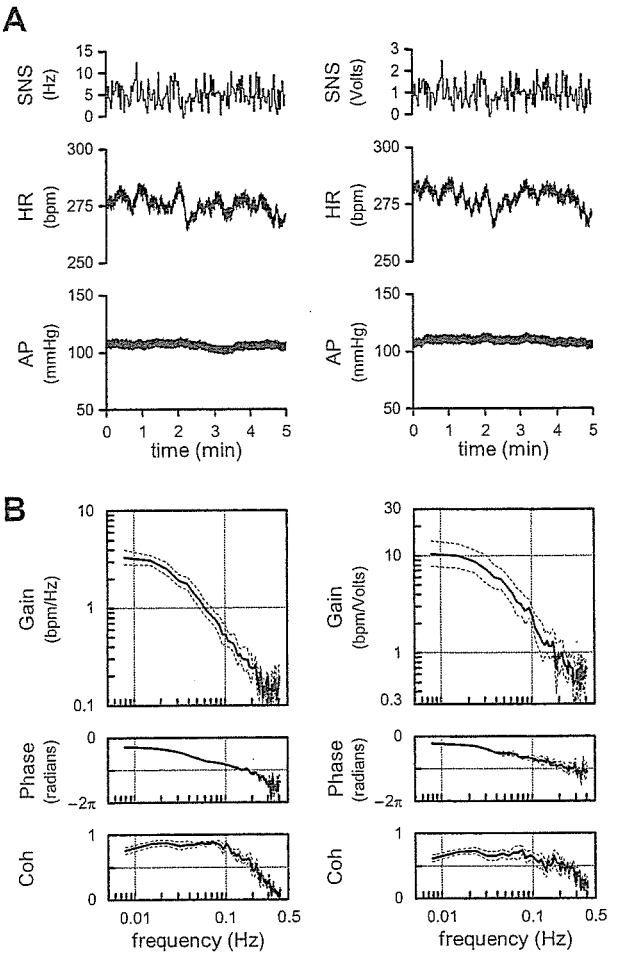

Fig. 7. **A**: Time series of SNS, HR, and AP using frequency modulation (left) and amplitude modulation (right) as the input signal. HR changed dynamically in response to both the frequency modulation and amplitude modulation of SNS. **B**: Averaged transfer functions obtained from 5 animals using frequency modulation (left) and amplitude modulation (right) as the input signal. Although the absolute gain values are different because of different units in inputs, the low-pass characteristics are in common for both transfer functions.

APPENDIX A

Frequency modulation versus amplitude modulation in nerve stimulation. Because the sinus node responds to NA released from the sympathetic nerve terminals and because the NA kinetics at the neuroeffector junction predominantly determine the low-pass filter characteristics of the HR response to SNS [12], whether the SNS is modulated by frequency or amplitude will not significantly affect the transfer function from SNS to HR. Although the frequency modulation and the amplitude modulation would reveal different nonlinear input-output relationships between the stimulation command signal and the number of nerve fibers actually discharged, a transfer function analysis using a white noise input can retrieve a linear input-output relationship even in the presence of a significant nonlinearity [11]. Although the SNS we used is different from a physiological discharge of nerve fibers, the HR response to physiological nerve discharge would obey the same principle characterized by the transfer function from SNS to HR. When we estimated the transfer function from recorded sympathetic nerve activity to HR, it also approximates to the second-order low-pass filter with pure dead time [25].

We compared the transfer function from SNS to HR identified by the frequency-modulation input and that by the amplitude-modulation input in 5 anesthetized rabbits. The left panel of Fig. 7A shows a typical time series of SNS, HR, and AP obtained from the frequency-modulation input with a constant amplitude of 3 V (2-ms pulse width, 2-s switching interval). The right panel of Fig. 7A shows the time series obtained from the amplitude-modulation input with a constant frequency of 5 Hz (2-ms pulse width, 2-s switching interval). Figure 7B summarizes the averaged transfer function obtained by the frequency-modulation input (left panel) and that by the amplitude-modulation input (right panel). Although the units of gain differ between the two, general low-pass characteristics were in common. The coherence values associated with

the amplitude-modulation input seems smaller than those associated with the frequency-modulation input. In regard to the amplitude-modulation input, the stimulation amplitude usually crosses the threshold amplitude, below which the nerve fibers do not discharge. Such a nonlinear process of the amplitude-modulation input would contribute to the lower coherence values.

APPENDIX B

A mathematical modeling of dynamic heart rate response to sympathetic nerve stimulation using a second-order low-pass filter with pure dead time. We adopted a mathematical model of a second-order low-pass filter with pure dead time to quantify the transfer function from SNS to HR. In the left panel of Fig. 8, the thick line represents a typical transfer function obtained under the NA_0 condition in one animal. The thin smooth curve represents a best-fit mathematical model. A schematic explanation of the model parameters is shown in the right panel of Fig. 8. The dynamic gain, K, determines the value the transfer gain approaches as the frequency goes to zero. The natural frequency, f_N, determines the frequency of low-pass characteristics. The phase of the second-order low-pass filter delays by $\pi/2$ radians at f_N when the pure dead time is zero. The damping ratio, ζ, determines how fast the transfer gain wanes around f_N. As an example, the gain plot shows a slight peaking around f_N when $\zeta = 0.5$. On the other hand, the gain plot shows a more gradual decrease around f_N when $\zeta = 2.0$. The maximum phase delay of the second-order low-pass filter is π radians. The pure dead time, L, determines the additional phase delay necessary for explaining the phase difference between the measured transfer function and the second-order low-pass filter.

This study was supported by "Health and Labour Sciences Research Grant for Research on Advanced Medical Technology" from the Ministry of Health, Labour and Welfare of Japan; "Health and Labour Sciences Research Grant for Research on Medical Devices for Analyzing, Supporting and Substituting the Function of Human Body" from the Ministry of Health, Labour and Welfare of Japan; "Health and Labour Sciences Research Grant H18-Iryo-Ippan-023" from the Ministry of Health, Labour and Welfare of Japan; "Program for Promotion of Fundamental Studies in Health Science" from the National Institute of Biomedical Innovation, a grant provided by the Ichiro Kanehara Foundation; "Ground-based Research Announcement for Space Utilization" promoted by the Japan Space Forum; and "Industrial Technology Research Grant Program in 03A47075" from the New Energy and Industrial Technology Development Organization (NEDO) of Japan.

REFERENCES

1. Kawada T, Fujiki N, Hosomi H. Systems analysis of the carotid sinus baroreflex system using a sum-of-sinusoidal input. Jpn J Physiol. 1992;42:15-34.
2. Kawada T, Yamamoto K, Kamiya A, Ariumi H, Michikami D, Shishido T, Sunagawa K, Sugimachi M. Dynamic characteristics of carotid sinus pressure-nerve activity transduction in rabbits. Jpn J Physiol. 2005;55:157-63.
3. Kawada T, Ikeda Y, Sugimachi M, Shishido T, Kawaguchi O, Yamazaki T, Alexander J Jr, Sunagawa K. Bidirectional augmentation of heart rate regulation by autonomic nervous system in rabbits. Am J Physiol Heart Circ Physiol. 1996;271:H288-95.
4. Kawada T, Sugimachi M, Shishido T, Miyano H, Ikeda Y, Yoshimura R, Sato T, Takaki H, Alexander J Jr, Sunagawa K. Dynamic vagosympathetic interaction augments heart rate response irrespective of stimulation patterns. Am J Physiol Heart Circ Physiol. 1997;272:H2180-7.
5. Cryer PE. Physiology and pathophysiology of the human sympathoadrenal neuroendocrine system. N Eng J Med. 1980;303:436-44.
6. Langer SZ, Adler-Graschinsky E, Giorgi O. Physiological significance of α-adrenoceptor-mediated negative feedback mechanism regulating noradrenaline release during nerve stimulation. Nature. 1977;265:648-50.
7. Majewski H, Rand MJ, Tung LH. Activation of prejunctional β-adrenoceptors in rat atria by adrenaline applied exogenously or released as a co-transmitter. Br J Pharmacol. 1981;73:669-79.
8. Honda T, Ninomiya I, Azumi T. Cardiac sympathetic nerve activity and catecholamine kinetics in cat hearts. Am J Pysiol Heart Circ Physiol. 1987;252:H879-85.
9. Brigham EO. The Fast Fourier Transform and Its Applications. Englewood Cliffs, NJ: Prentice-Hall; 1988. p. 167-203.
10. Bendat JS, Piersol AG. Random Data Analysis and Measurement Procedures. 3rd ed. New York: John Wiley & Sons; 2000. p. 189-217.
11. Marmarelis PZ, Marmarelis VZ. Analysis of Physiological Systems. New York: Plenum; 1978. p. 131-221.
12. Nakahara T, Kawada T, Sugimachi M, Miyano H, Sato T, Shishido T, Yoshimura R, Miyashita H, Inagaki M, Alexander J Jr, Sunagawa K. Neuronal uptake affects dynamic characteristics of heart rate response to sympathetic stimulation. Am J Physiol Regul Integr Comp Physiol. 1999;277:R140-6.
13. Glantz SA. Primer of Biostatistics (5th ed). New York: McGraw-Hill; 2002.
14. Young MA, Hintze TH, Vatner SF. Correlation between cardiac performance and

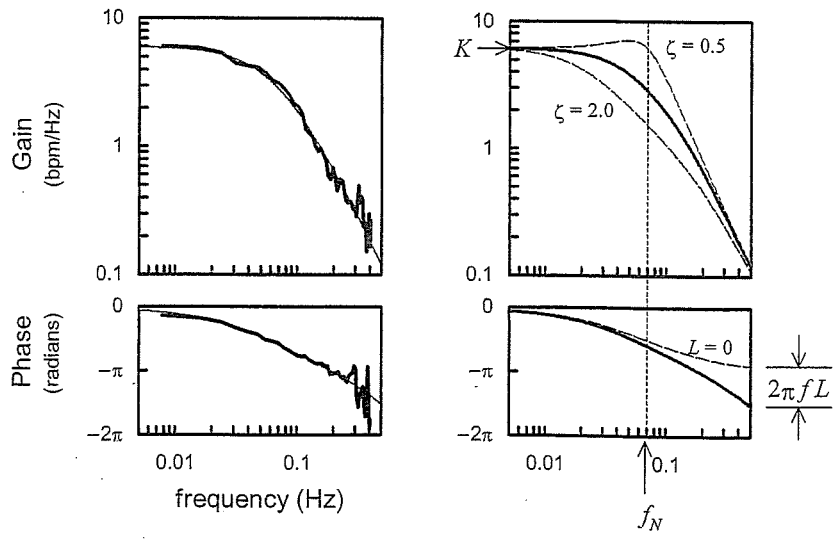

Fig. 8. A: Typical transfer function from SNS to HR obtained under control conditions (NA_0) in one animal. The thin smooth curve is a best-fit mathematical model for the transfer function. **B**: Schematic explanation of the model parameters. K: dynamic gain; f_N: natural frequency; ζ: damping ratio; L: pure dead time.

plasma catecholamine levels in conscious dogs. Am J Physiol Heart Circ Physiol. 1985;248:H82-8.
15. Novi AM. An electron microscope study of the innervation of papillary muscles in the rat. Anat Rec. 1968;160:123-41.
16. Yamaguchi N, de Champlain J, Nadeau R. Correlation between the response of the heart to sympathetic stimulation and the release of endogenous catecholamines into the coronary sinus of the dog. Circ Res. 1975;36:662-8.
17. Kawada T, Yamazaki T, Akiyama T, Shishido T, Miyano H, Sato T, Sugimachi M, Alexander J Jr, Sunagawa K. Interstitial norepinephrine level by cardiac microdialysis correlates with ventricular contractility. Am J Physiol Heart Circ Physiol. 1997;273:H1107-12.
18. Iversen LL. The uptake of catechol amines at high perfusion concentrations in the rat isolated heart: a novel catecholamine uptake process. Brit J Pharmacol. 1965;25:183-33.
19. Iversen LL. Uptake processes for biogenic amines. In: Iversen LL, Iversen SD, Snyder SH, editors. Handbook of Psychopharmacology, Section 1, Vol 3. New York: Plenum Press; 1975. p. 381-442.
20. Friedgen B, Halbrügge T, Graefe K. Role of uptake$_1$ and catechol-O-methyltransferase in removal of circulating catecholamines in the rabbit. Am J Physiol Endocrinol Metab. 1994;267:E814-21.
21. Boudreau G, Péronnet F, de Champlain J, Nadeau R. Presynaptic effects of epinephrine on norepinephrine release from cardiac sympathetic nerves in dogs. Am J Physiol Heart Circ Physiol. 1993;265:H205-11.
22. Esler M, Jennings G, Lambert G, Meredith I, Horne M, Eisenhofer G. Overflow of catecholamine neurotransmitters to the circulation: source, fate, and functions. Physiol Rev. 1990;70:963-85.
23. Schmidt H, Schurr C, Hedler L, Majewski H. Local modulation of norepinephrine release in vivo: Presynaptic β_2-adrenoceptors and endogenous adrenaline. J Cardiovasc Pharmacol. 1984;6:641-9.
24. Kawada T, Sugimachi M, Shidhido T, Miyano H, Sato T, Yoshimura R, Miyashita H, Nakahara T, Alexander J Jr, Sunagawa K. Simultaneous identification of static and dynamic vagosympathetic interactions in regulating heart rate. Am J Physiol Regul Integr Comp Physiol. 1999;276:R782-9.
25. Kawada T, Miyamoto T, Uemura K, Kashihara K, Kamiya K, Sugimachi M, Sunagawa K. Effects of neuronal norepinephrine uptake blockade on baroreflex neural and peripheral arc transfer characteristics. Am J Physiol Regul Integr Comp Physiol. 2004;286:R1110-20.